The Journal of Chemical Physics

RESEARCH ARTICLE | AUGUST 26 2024

Issues with lipid probes in flip-flop measurements: A comparative study using sum-frequency vibrational spectroscopy and second-harmonic generation

Special Collection: Festschrift in honor of Yuen-Ron Shen

Joshua M. Taylor ; John C. Conboy

Check for updates

J. Chem. Phys. 161, 085104 (2024)
https://doi.org/10.1063/5.0226075

View Online
Export Citation

19 December 2024 21:33:17

AIP Publishing
The Journal of Chemical Physics
Special Topics Open for Submissions
Learn More

AIP Publishing

The Journal of Chemical Physics ARTICLE pubs.aip.org/aip/jcp

Issues with lipid probes in flip-flop measurements: A comparative study using sum-frequency vibrational spectroscopy and second-harmonic generation

Cite as: J. Chem. Phys. 161, 085104 (2024); doi: 10.1063/5.0226075
Submitted: 28 June 2024 • Accepted: 11 August 2024 •
Published Online: 26 August 2024

View Online Export Citation CrossMark

Joshua M. Taylor and John C. Conboy[a)]

AFFILIATIONS

Department of Chemistry, University of Utah, 315 South 1400 East RM. 2020, Salt Lake City, Utah 84112, USA

Note: This paper is part of the JCP Festschrift in Honor of Yuen-Ron Shen.
[a)]**Author to whom correspondence should be addressed:** John.Conboy@utah.edu

ABSTRACT

Fluorescent lipid probes such as 1-palmitoyl-2-(6-[7-nitro-2-1,3-benzoxadiazol-4-yl]amino-hexanoyl)-sn-*glycero*-3-phosphocholine (C6 NBD-PC) have been used extensively to study the kinetics of lipid flip-flop. However, the efficacy of these probes as reliable reporters of native lipid translocation has never been tested. In this study, sum-frequency vibrational spectroscopy (SFVS) was used to measure the kinetics of C6 NBD-PC lipid flip-flop and the flip-flop of native lipids in planar supported lipid bilayers. C6 NBD-PC was investigated at concentrations of 1 and 3 mol. % in both chain-matched 1,2-dipalmitoyl-sn-*glycero*-3-phosphocholine (DPPC) and chain-mismatched 1,2-distearoyl-sn-*glycero*-3-phosphocholine (DSPC) to assess the ability of C6 NBD-PC to mimic the behavior of the surrounding matrix lipids. It was observed that C6 NBD-PC exhibited faster flip-flop kinetics compared to the native lipids in both DPPC and DSPC matrices, with notably accelerated rates in the chain-mismatched DSPC system. SFVS was also used to measure the acyl chain orientation and gauche content of C6 NBD-PC in both DPPC and DSPC membranes. In the DSPC matrix (chain mismatched), C6 NBD-PC was more disordered in terms of both gauche content and acyl tilt, whereas it maintained an orientation similar to that of the native lipids in the DPPC matrix (chain matched). In addition, the flip-flop kinetics of C6 NBD-PC were also measured using second-harmonic generation (SHG) spectroscopy, by probing the motion of the NBD chromophore directly. The flip-flop kinetics measured by SHG were consistent with those obtained from SFVS. This study also marks the first instance of phospholipid flip-flop kinetics being measured via SHG. The results of this study clearly demonstrate that C6 NBD-PC does not adequately mimic the behavior of native lipids within a membrane. These findings also highlight the significant impact of the lipid matrix on the flip-flop behavior of the fluorescently labeled lipid, C6 NBD-PC.

Published under an exclusive license by AIP Publishing. https://doi.org/10.1063/5.0226075

19 December 2024 21:33:17

INTRODUCTION

Scientists have extensively researched the plasma membrane in recent decades to gain a deeper understanding of this intricate barrier, which separates cells from their external environment. There is a particular interest in lipid flip-flop dynamics that govern the creation and maintenance of lipid asymmetry in a cell's membrane.[1–7] It has been commonly proposed that flip-flop is an enzymatically driven process that involves the unidirectional movement of a phospholipid from one leaflet to the other through the use of phospholipid-specific, ATP driven "flippases" and "floppases."[8–11] Protein-free, or intrinsic lipid flip-flop, has been observed in the absence of flippases and floppases, though the rate, mechanism, and biological relevance are currently under heavy debate.

The complexities associated with the measurement of native lipid flip-flop in living cells make it difficult to measure the process in a reliable manner. As such, model membranes including vesicles or planar supported lipid bilayers (PSLBs) are commonly used to infer how phospholipids flip and flop in the absence of proteins.

Published under an exclusive license by AIP Publishing

The first ever attempt to measure the rate of native lipid flip-flop was the pioneering work of Kornberg and McConnell with the use of electron paramagnetic resonance (EPR).[12] A mixture of egg PC and (2,2,6,6-tetramethylpiperidin-1-yl)oxyl–1,2-dipalmitoyl-sn-3-*glycero*-phosphocholine (TEMPO-DPPC) was used to create vesicles containing a symmetric distribution of TEMPO-DPPC in the inner and outer leaflets. The rate of TEMPO-DPPC flip-flop was measured by first reducing the outer leaflet TEMPO-DPPC with sodium ascorbate and tracking the subsequent ESR signal decay due to the inner leaflet TEMPO-DPPC flopping outward to interact with sodium ascorbate in solution.[12] Kornberg and McConnell found that the half-life of flip-flop for TEMPO-DPPC was on the order of hours at 30 °C in an egg PC matrix, which was concluded to be too slow to be of any biological importance. Over the years, a multitude of other methods have been developed to study flip-flop, including fluorescence,[13–17] neutron reflectometry (NR) and small angle neutron scattering (SANS),[18,19] proton nuclear magnetic resonance (^{1}H NMR),[20] and sum-frequency vibrational spectroscopy (SFVS),[21] which have produced varying results, leading to no consensus on what method captures the "true" flip-flop rate.

Of those methods discussed above, one of the more popular methods is fluorescence spectroscopy. The sensitivity of fluorescence allows for a lower concentration of the labeled lipid to be used, a critical factor to consider when working with bulky labels that can perturb the membrane. Flip-flop experiments using fluorescently probed lipids typically rely on the quenching of the fluorophore on the outer leaflet of the membrane and measuring the additional loss of fluorescence as the inner leaflet fluorescent lipids flop to the outer leaflet and are subsequently quenched. While there are a variety of fluorescent labels that can be attached to lipids, nitrobenzoxadiazole (NBD) is among the most popular fluorophores used given its relatively small size and its incredible sensitivity to its environment, being weakly fluorescent in water but highly fluorescent in hydrophobic environments, making it especially suitable for membrane studies.[22–25] Transbilayer movement has been studied in both vesicle and cell systems using NBD labeled lipids such as 1-palmitoyl-2-(6-[7-nitro-2-1,3-benzoxadiazol-4-yl]amino-hexanoyl)-sn-*glycero*-3-phosphocholine (C6 NBD-PC) among other NBD labeled lipid analogs.[13–17] These NBD lipid analogs can vary in chain length, phospholipid headgroup, and the placement of the NBD label (fatty acid or headgroup modified); however, the short chain analog C6 NBD-PC is one of the most commonly used, which is exclusively labeled on the *sn*2 chain.[26] These fluorescence experiments have generally shown native flip-flop to be a slow process, with a few exceptions suggesting that flip-flop can approach accelerated rates at elevated temperatures near the phase transition of the lipid.[17] In particular, John *et al.* found that small unilamellar vesicles (SUVs) composed of 1,2-dipalmitoyl-sn-*glycero*-3-phosphocholine (DPPC) or 1,2-dimyristoyl-sn-*glycero*-3-phosphocholine (DMPC) containing 1 mol. % C6 NBD-PC had flip-flop half-lives of only a few minutes at and above the phase transition temperature of DPPC and DMPC, with the fastest rates occurring at the phase transition, ~9 and 2 min for DPPC and DMPC vesicles at 41 and 23 °C, respectively.[17] John *et al.* also observed no change in fluorescence signal below the phase transition temperature and concluded that gel phase lipids such as DPPC and DMPC do not readily flip-flop but flip-flop rapidly in the liquid-crystalline phase.

While the initial flip-flop studies conducted with ESR and fluorescence were some of the first successful attempts to measure lipid translocation and set a historical benchmark, criticisms have been made on the use of labeled lipids in measuring flip-flop kinetics. The most commonly expressed argument against the use of probes is the addition of bulky labels that not only change the size but also the chemical properties of the lipids, which could significantly influence the energetics of the process and therefore the rate at which flip-flop occurs. Regardless of this criticism, labeled lipids, fluorescently labeled lipids in particular, are still a very popular means of tracking and determining a variety of kinetic phenomena in membrane systems with lipid flip-flop being a specific example of this. A counter argument that has been made is that if the probe is at low enough concentrations, it should not have a meaningful impact on the membrane as a whole and should behave similar to its matrix. However, fluorescence experiments have an inability to distinguish the rates of the fluorescently labeled lipid from the label-free parent lipid matrix. This does not allow for experiments to verify that the probe behaves like its parent lipid matrix and by extension an inability to determine whether the probe causes disruption to the membrane, leading to different kinetics in the presence or absence of the probe. In addition, the claim that low concentrations of the probe do not perturb the membrane sets a vague benchmark for what is considered a "low enough" concentration. There is a general agreement that 1 mol. % NBD and less is considered a sufficiently low concentration to prevent self-quenching of the fluorophore while also minimizing the perturbation of the membrane,[23] although examples of concentrations as high as 5 mol. % NBD are found throughout the literature.[22,27,28] Interestingly, differential scanning calorimetry of DPPC vesicle systems containing C6 NBD-PC and 1-palmitoyl-2-[12-(7-nitrobenz-2-oxa-1,3-diazol-4-yl)aminododecanoyl]-sn-*glycero*-3-phosphocholine (C12 NBD-PC) has shown that 0.6 mol. % C6 NBD-PC is enough to alter the phase transition temperature of DPPC vesicles, while at 0.25 mol. %, C12 NBD-PC causes an even more significant perturbation, suggesting that this 1 mol. % standard may be invalid.[29]

The issues that occur when working with labeled lipids have motivated some groups to use label-free methods that eliminate the use of bulky labels. These methods typically require the use of deuterated analogs of native lipids that do not chemically change the nature of the lipid in the membrane. These label-free methods include neutron scattering techniques such as NR[18] and SANS[19] as well as methods such as ^{1}H NMR[20] and SFVS.[21] Methods such as SANS use elastic neutron scattering on proteated and deuterated vesicles, which have unique scattering length densities (SLDs). As these vesicles begin to interact through inter-vesicle exchange and subsequently flip-flop, it is observed that mixed vesicles give SLDs similar to that of the solvent (contrast matched) providing a baseline for complete inter-vesicle exchange and flip-flop. This allows for the determination of the rate of inter-vesicle exchange and flip-flop by looking at the contrast decay from proteated and deuterated vesicles to that of the mixed vesicles. Unfortunately, these methods are not capable of distinguishing between the rate of inter-vesicle exchange and flip-flop rates, leading to an assumption of flip-flop being the slow or rate limiting step. In addition, neutron scattering methods are known to have long data acquisition (DAQ) times, making real-time analysis of lipid translocation, whose rate is still

19 December 2024 21:33:17

Published under an exclusive license by AIP Publishing

under debate, an issue. ^{1}H NMR relies on distinguishing the inner and outer leaflets of vesicles through the use of lanthanide shift reagents (LSRs). Asymmetric vesicles with isotopically unique lipids in the inner and outer leaflets are created by methyl-β-cyclodextrin (MβCD) facilitated exchange, and the subsequent mixing of these lipids can be used to determine the rate of flip-flop.[20] For example, in Marquardt's work, MβCD was used to transfer headgroup-labeled DPPC (DPPC-d13) to an acceptor vesicle population containing tail-labeled DPPC (DPPC-d62) to create vesicles with DPPC-d13 exclusively on the outer leaflet and DPPC-d62 on the inner leaflet giving a unique signal when using a LSR, which only shifts the outer leaflet.[20] As flip-flop occurs, the LSR would shift the signal associated with the DPPC-d62, now in the outer leaflet, allowing for the determination of the rate of flip-flop with this change in signal. Marquardt *et al.* found that the half-life of DPPC flip-flop was on the order of hours to days, even in the fluid phase.[20]

Our group has studied the flip-flop rates of native lipids using SFVS, a coherent, second-order, nonlinear optical technique that relies on the asymmetric distribution of proteated and deuterated lipids to determine the rate of flip-flop.[21] SFVS is a powerful technique as it has the ability to measure native lipid flip-flop, as well as labeled lipids, through the vibrational modes of the lipids themselves. This approach allows for the independent measurement of native lipids and labeled lipids to determine if the flip-flop rates of these species differ. The extent to which labeled-lipids influence the native lipid flip-flop dynamics can also be determined. Our group has shown that the flip-flop kinetics of the head labeled TEMPO-DPPC used in Kornberg and McConnell's work are significantly different than the native DPPC lipid it is assumed to mimic, with a half-life ~46 times slower than the native lipid at 37 °C.[30] In addition to probing flip-flop kinetics, SFVS is also capable of determining the orientation of lipids within the membrane.[31] This gives SFVS a unique advantage to not only study the flip-flop kinetics of labeled lipids and compare them to their native counterparts, but also provides insight into how labeled lipids orient themselves within the membrane and how they could potentially influence the ordering of the membrane as a whole. SFVS experiments can tackle important questions about the use of labeled lipids, such as whether these labeled lipids accurately represent native phospholipids in addition to providing insights into the impact the labeled lipids have on the lipid membrane.

In this study, the flip-flop kinetics of C6 NBD-PC were investigated to determine if the lipid probe C6 NBD-PC behaves similarly to the parent lipid matrix. In the current study, we have looked at C6 NBD-PC at a low concentration (1 mol. %) and a high concentration (3 mol. %) in a chain length matching DPPC matrix and a chain length mismatching DSPC matrix. These lipids and their deuterated analogs can be seen in Fig. 1. In addition to flip-flop kinetics, the orientation of the alkyl chains of both C6 NBD-PC and native lipids was examined via SFVS in order to investigate the structure perturbation of C6 NBD-PC on the membrane. Alongside SFVS, second-harmonic generation (SHG) was employed as a complementary technique to specifically probe the NBD moiety. This allows for two distinct measurements of different portions of C6 NBD-PC. These studies are meant to address the following questions: Are the rates of flip-flop for C6 NBD-PC and the unmodified lipids of the membrane the same? What effect does the concentration or mole fraction of C6 NBD-PC have on the flip-flop kinetics of both the probe and native lipid species in the membrane? Finally, are there structural perturbations induced in the parent lipid matrix upon the addition of C6 NBD-PC? The answers to these questions will go a long way in addressing some of the discrepancies observed in the reported flip-flop rates of labeled lipid species vs their unlabeled counterparts and would either justify the use or avoidance of these labeled lipids.

Sum-frequency vibrational spectroscopy theory

Sum-frequency vibrational spectroscopy (SFVS) and nonlinear optics as a whole has its beginnings in the 1960s where initial theoretical and experimental examination of nonlinear phenomena was explored by Bloembergen.[32–35] Bloembergen went on to share the Nobel Prize in Physics in 1981 for his contributions to the field of nonlinear optics and laser spectroscopy. In the 1980s, invaluable contributions were made by one of Bloembergen's students, Shen, who was the first scientist to demonstrate sum-frequency generation as a powerful surface selective vibrational spectroscopic technique by collecting SFVS spectra of monolayers at a variety of surfaces.[36–38] Shen's initial studies, as well as his continuing contribution to the field of nonlinear optics, have revolutionized the study of surface science, and the wealth of knowledge gained about the physical and chemical nature of interfaces cannot be overstated. Through Shen's foundational work, as well as the work of numerous others, the characterization of molecules at interfaces as well as kinetic measurements such as flip-flop can readily be examined through the use of SFVS.

SFVS at bilayer interfaces

SFVS is a label-free technique that has been extensively used for studying phospholipids in model membranes in a noninvasive manner.[21,30,39–49] The theoretical underpinnings of SFVS are described in detail within other literature,[50] and only a brief description will be provided here. SFVS is a coherent second-order nonlinear scattering technique that is allowed only in systems where inversion symmetry is absent. Because of this, SFVS does not occur in bulk centrosymmetric materials but is allowed at interfaces where the inversion symmetry of the bulk material is broken. Sum-frequency vibrational spectra are generated by spatially and temporally overlapping a visible laser source with a tunable infrared laser source. This spatial and temporal overlap yields photons at the sum of the two incoming photon frequencies,

$$\omega_{SF} = \omega_{vis} + \omega_{IR}, \tag{1}$$

and the intensity of the sum-frequency is described by

$$I_{SF} = \left| \tilde{f}_{SF} f_{vis} f_{IR} \chi^{(2)} \right|^2, \tag{2}$$

where $\tilde{f}_{SF}$ is the nonlinear geometric Fresnel coefficient, f_{vis} and f_{IR} are the geometric Fresnel coefficients for the visible and IR beams, respectively, and $\chi^{(2)}$ is the second-order nonlinear susceptibility tensor.[50,51] $\chi^{(2)}$ is the sum of both the resonant ($\chi_R^{(2)}$) and nonresonant ($\chi_{NR}^{(2)}$) susceptibilities,

$$\chi^{(2)} = \chi_R^{(2)} + \chi_{NR}^{(2)}. \tag{3}$$

19 December 2024 21:33:17

Published under an exclusive license by AIP Publishing

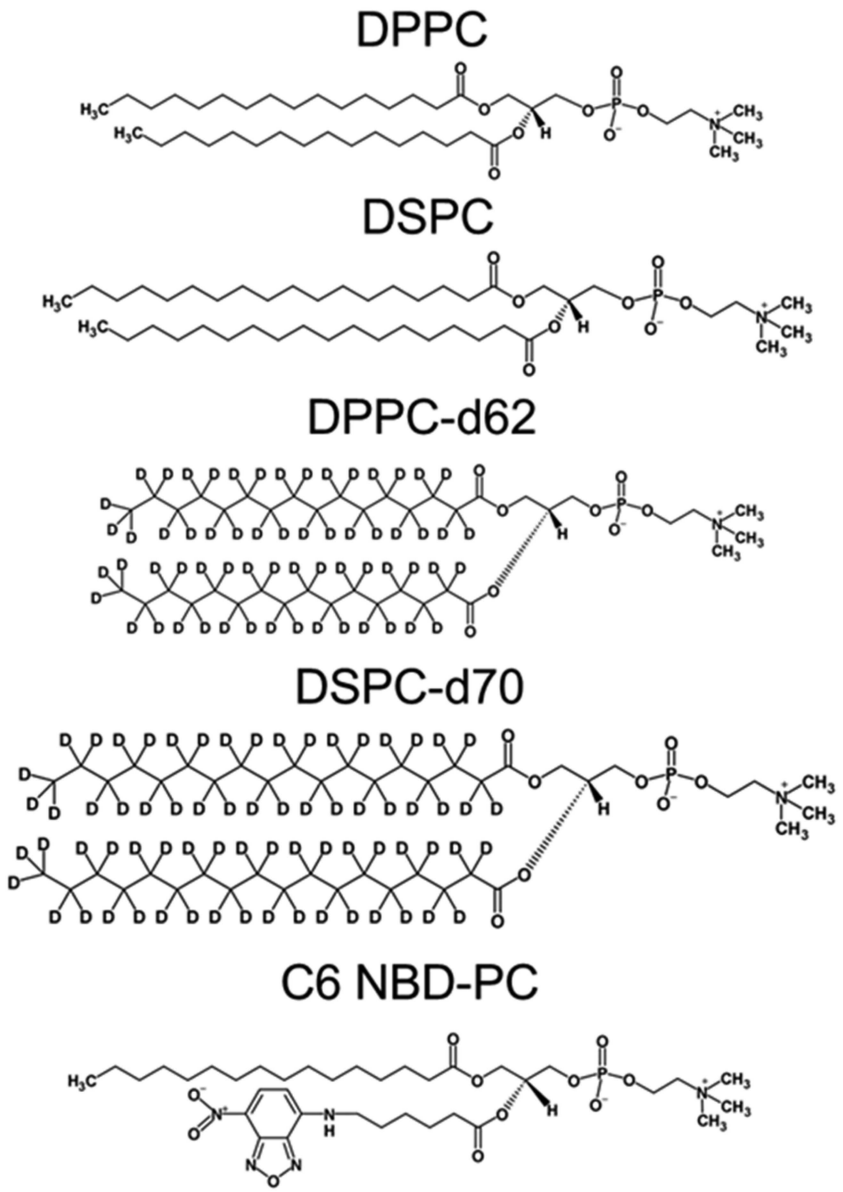

FIG. 1. Molecular structures of DPPC, DSPC, DPPC-d62, DSPC-d70, and C6 NBD-PC.

The nonresonant contribution is negligible in dielectric materials and can often be ignored. The resonant contribution to $\chi^{(2)}$ is described by the following equation:

$$\chi_R^{(2)} = \sum_v \frac{N\langle A_i M_{jk}\rangle}{\omega_v - \omega_{IR} - i\Gamma_v}, \tag{4}$$

where N is the number of SHG active molecules, A_i is the IR transition probability, M_{jk} is the Raman transition probability, ω_v is the frequency of a vibrational mode at the surface, ω_{IR} is the frequency of the IR field, and Γ_v is the linewidth of the transition. Examination of Eq. (4) reveals that in order to observe sum-frequency, a transition must be both IR and Raman active and that a maximum signal intensity is observed when on resonance with a vibrational frequency (ω_v) that is present on the surface. SFVS is also extremely sensitive to the relative orientation of the transition dipole moments being probed at the surface. This characteristic is taken advantage of by carefully considering the polarization states of the incident electric fields. Similar to IR spectroscopy, vibrational modes parallel and perpendicular to surface normal can be examined by changing the polarization of the incoming IR electric field. In SFVS, the

19 December 2024 21:33:17

Published under an exclusive license by AIP Publishing

examination of vibrational transitions parallel to surface normal can be accomplished using the polarization combination of s-polarized sum-frequency, s-polarized visible, and p-polarized IR (*ssp*), while transitions perpendicular to surface normal are measured using s-polarized sum-frequency, p-polarized visible, and s-polarized IR (*sps*).[30] Our group has demonstrated that when using *ssp* polarization on asymmetric lipid bilayers, a large sum-frequency signal is generated from the terminal methyl symmetric stretch (CH_3 ν_s) of the acyl chains at a frequency of 2876 cm^{-1}. The prominence of this vibrational mode is due to the transition dipole moments of the terminal methyl group being oriented nearly parallel to the surface normal.[31] However, in a normal phospholipid bilayer, these terminal methyl groups, as well as every other observable vibrational mode, are present in each leaflet, which results in the bilayer having equal but opposing dipole moments. Due to the symmetry requirements of sum-frequency generation, these opposing dipoles lead to destructive interference and a net cancellation of the sum-frequency signal. Selective deuteration of one leaflet of the bilayer, however, creates a bilayer in which this net cancellation is removed due to the shifted vibrational frequencies of the C–D transitions in the opposing leaflet, making the bilayer sum-frequency active. This selective deuteration can be accomplished through the use of planar supported lipid bilayers (PSLBs) and the Langmuir–Blodgett/Langmuir–Schaefer (LB/LS) deposition methods (discussed below). Through the use of PSLBs, the probing of both native lipids and lipid probes, such as C6 NBD-PC, can be accomplished. With C6 NBD-PC in particular, the probing of the terminal methyl group of the alkyl chain lacking the NBD label allows for the measurement of the labeled lipid without needing to probe the NBD molecule in particular, avoiding the use of quenching reagents associated with traditional fluorescence experiments.

Orientation measurements by SFVS

A useful aspect of SFVS is its ability to determine the orientation of the alkyl chains of the phospholipids within the membrane. SFVS spectra of different polarization states in conjunction with Raman depolarization data can be used to measure the terminal methyl group tilt angle of lipids in PSLBs.[31] This is accomplished by comparing the relative amplitudes of the SFVS signal of the CH_3 ν_s mode at 2876 cm^{-1} with *ssp* (s-polarized sum-frequency, s-polarized visible, and p-polarized IR) and *sps* (s-polarized sum-frequency, p-polarized visible, and s-polarized IR) polarization combinations. The *ssp* polarization state probes vibrational modes parallel to surface normal, while an *sps* polarization state probes the planes perpendicular to surface normal and by extension perpendicular to the membrane. The relative SFVS signal amplitudes, after correcting using the Fresnel coefficients, can be used to determine the tilt angle (θ) of the terminal methyl group relative to the surface normal. This methyl tilt angle is calculated by assuming a delta function distribution using the following equation:[52,53]

$$\theta = \arccot\left[\left(\frac{\chi^{(2)}_{ssp}}{\chi^{(2)}_{sps}} - \frac{1+R}{1-R}\right)\frac{1-R}{2R}\right]^{\frac{1}{2}}, \tag{5}$$

where $\chi^{(2)}_{ssp}$ is the second order susceptibility tensor with s-polarized sum-frequency, s-polarized visible, and p-polarized IR and $\chi^{(2)}_{sps}$ is the second order susceptibility tensor with s-polarized sum-frequency, p-polarized visible, and s-polarized IR. The value R is described by

$$R = \frac{Q-1}{Q+2} or \frac{Q+1}{Q-2},\ where\ Q = \left[\frac{3}{5}\left(\frac{1}{\rho} - \frac{4}{3}\right)\right]^{\frac{1}{2}}, \tag{6}$$

where ρ is the Raman depolarization ratio, an experimentally determined value, which has been found to be 0.023 for CH_3 ν_s.[52] Which value R takes on is determined by the ratio between $\chi^{(2)}_{ssp}$ and $\chi^{(2)}_{sps}$. If the ratio is positive, an R value less than one must be selected, while if the ratio is negative, R larger than one is selected.[53] $\chi^{(2)}_{ssp}$ and $\chi^{(2)}_{sps}$ can be determined by the following equations:

$$\chi^{(2)}_{ssp} = \left(\frac{A_{ssp}}{\left|\tilde{f}^{SF}_{y} f^{vis}_{y} f^{IR}_{z}\right|^2}\right)^{\frac{1}{2}}, \tag{7}$$

$$\chi^{(2)}_{sps} = \left(\frac{A_{sps}}{\left|\tilde{f}^{SF}_{y} f^{vis}_{z} f^{IR}_{y}\right|^2}\right)^{\frac{1}{2}}, \tag{8}$$

where A_{ssp} and A_{sps} are the sum-frequency amplitudes of the CH_3 ν_s mode, which are determined by the fitted peaks of the SFVS spectra, $\tilde{f}^{SF}$ is the nonlinear geometric Fresnel coefficient, and f^{vis} and f^{IR} are the geometric Fresnel coefficients for the visible and IR beams, respectively.[50,51] It has been determined previously for PSLBs that the methyl group angle and the corresponding alkyl chain tilt angle were 22° ± 4° and 13° ± 4°, respectively, which is in good agreement with both molecular dynamic simulations and experimental studies using neutron reflectometry and x-ray diffraction.[54–59] With the tilt angle, one can gain a good description of the overall chain ordering within the bilayer of both C6 NBD-PC and the parent lipid matrix to determine if the introduction of the labeled lipid generates significant disorder within the bilayer. In addition to the measuring of tilt angles, a semi-quantitative description of the gauche content can be found using the ratio of the calculated amplitudes of the methylene symmetric stretch (CH_2 ν_s) to CH_3 ν_s, which will be discussed further in the Results and Discussion section.

Flip-flop kinetics measured by SFVS

As previously mentioned, SFVS measurements of lipid flip-flop rely on the partial deuteration of PSLBs and do not rely on the use of bulky fluorescent probes such as those methods previously discussed.[13–17] When flip-flop of these asymmetric PSLBs begins, mixing of the proteated and deuterated lipids creates a gain in symmetry, or the canceling of dipole moments, causing destructive interference, leading to a signal decay over time. When examining the SFVS signal intensity from CH_3 ν_s in particular, the number difference of the CH_3 ν_s transitions in the proximal (N_{PROX}) and distal leaflets (N_{DIST}) of the PSLB leads to the following expression:

$$I_{CH_3\nu_s} \propto (N_{PROX} - N_{DIST})^2. \tag{9}$$

The rate of lipid flip-flop is measured by observing the signal decay over time at a particular temperature and fitting the decay to the following equation:

19 December 2024 21:33:17

Published under an exclusive license by AIP Publishing

$$I_{CH_3\nu_s} = I_{max}e^{(-4kt)} + I_{min}, \tag{10}$$

where I_{max} is the initial signal intensity of a fully asymmetric bilayer, t is time, k is the rate constant for flip-flop, and I_{min} is a signal offset determined by the instrument system.[30] The amplitude of the decay corresponds to the square of the asymmetry in the membrane once the membrane reaches the temperature at which collection of the decay begins. As lipid flip-flop will occur while the membrane is brought to the desired temperature, the raw decay data are normalized prior to fitting with Eq. (10). The half-life for lipid flip-flop can also be calculated from the rate constant using the following expression:

$$t_{\frac{1}{2}} = \frac{\ln(2)}{2k}. \tag{11}$$

The flip-flop rate constant at a particular temperature is also used to determine the free energy of activation ($\Delta G^{\ddagger}$) using the Eyring relation as follows:[60]

$$\Delta G^{\ddagger} = -RT\ln\left(\frac{kh}{k_B T}\right), \tag{12}$$

where k_B is the Boltzmann constant, T is temperature in kelvin, h is Planck's constant, and R is the gas constant. The transition state enthalpy ($\Delta H^{\ddagger}$) and entropy ($\Delta S^{\ddagger}$) for flip-flop can also be determined as a function of temperature using the Gibbs equation as follows:

$$\Delta G^{\ddagger} = \Delta H^{\ddagger} - T\Delta S^{\ddagger}. \tag{13}$$

Flip-flop kinetics measured by second-harmonic generation (SHG)

Similar to his work in SFVS, Shen's contribution to our understanding of SHG and its application at interfaces has also revolutionized surface science.[36,61] SHG is a second-order nonlinear optical technique that is generated when two incidental optical waves come in contact with a surface both spatially and temporally, producing a third wave at double the frequency,[50]

$$\omega_{SHG} = 2\omega, \tag{14}$$

where ω is the fundamental or driving frequency. The intensity of the SHG response is also dictated by the second-order susceptibility tensor, $\chi^{(2)}$, with its resonant portion expressed as

$$\chi^{(2)}_{ijk} = N\sum_{a,b,c}\frac{\langle a|\mu_i|c\rangle\langle a|\mu_j|b\rangle\langle b|\mu_k|c\rangle}{(2h\omega - E_{ac} - i\Gamma_{ca})(h\omega - E_{cb} - i\Gamma_{cb})}, \tag{15}$$

where N is the number of SHG active molecules; ω is the frequency of the incoming waves; h is Planck's constant; E is the energy of the optical transitions; Γ is the linewidth of the transition; and a, b, and c represent the initial, intermediate, and final states of the electronic transitions, respectively.[62,63] The subscripts i, j, and k of $\chi^{(2)}_{ijk}$ denote the input (j,k) and output (i) fields, which assume any of the three Cartesian coordinates (x,y,z). Similar to SFVS, SHG is sensitive to symmetry at the surface and similar asymmetry requirements are needed to observe SHG. Due to these similar requirements, it is possible to measure movement across a membrane such as phospholipid flip-flop using SHG if there are asymmetric electronic transitions within the membrane and a subsequent gain in symmetry. As such, the use of SHG to monitor kinetic events through membranes such as adsorption and molecular transport via SHG has been demonstrated in the literature over the years.[64–69] An example of this is the measurement of adsorption and subsequent transport kinetics of the SHG-active organic dye malachite green (MG) by Liu, Yan, and Eisenthal.[65] Similar to these transport studies using malachite green, SHG active molecules attached to a lipid, such as the NBD moiety on C6 NBD-PC lipids, are also capable of being probed and studied via SHG. If C6 NBD-PC is asymmetrically distributed within a PSLB, an SHG signal directly associated with the NBD molecule of the labeled lipid would be generated. As the labeled lipid begins to flip-flop, a gain of symmetry of the NBD moiety occurs, resulting in equal but opposite electronic transitions and a cancellation in the SHG signal, similar to the signal decay seen in SFVS. Equations (9)–(12) can therefore be applied to the cancellation of SHG signal as well and used to determine the rate of flip-flop, half-life, and activation energy of the labeled lipid specifically by measuring the SHG produced by the NBD label. The use of SHG to independently measure the flip-flop kinetics of C6 NBD-PC allows for a direct comparison with the previously published fluorescence data as both measurements rely on the NBD probe.

EXPERIMENTAL METHODS

Materials

All materials were used as received without further purification. 1,2-dipalmitoyl-sn-*glycero*-3-phosphocholine (DPPC), 1,2-dipalmitoyl-d62-sn-*glycero*-3-phosphocholine (DPPC-d62), 1,2-distearoyl-sn-3-*glycero*-phosphocholine (DSPC), 1,2-distearoyl-d70-sn-3-*glycero*-phosphocholine (DSPC-d70), and 1-palmitoyl-2-{6-[(7-nitro-2-1,3-benzoxadiazol-4-yl)amino]hexanoyl}-sn-*glycero*-3-phosphocholine (C6 NBD-PC) were purchased from Avanti Polar Lipids (Alabaster, AL). Sodium chloride, sodium hydroxide pellets, sulfuric acid, hydrochloric acid, and hydrogen peroxide were purchased from Fisher Chemical (Pittsburgh, PA). Sodium phosphate monohydrate (monobasic) and sodium phosphate heptahydrate (dibasic) were purchased from Mallinckrodt Chemicals (St. Louis, MO). Deuterium oxide, chloroform, and dithionite (85%) were purchased from Sigma-Aldrich Millipore (St. Louis, MO). All water used in these studies was obtained from a Barnstead Thermolyne (Dubuque, IA) Nanopure water system with a minimum resistivity of 18.2 MΩ cm. Phosphate buffered saline (PBS) was prepared using 150 mM NaCl, 5 mM $NaH_2PO_4 \cdot H_2O$, and 5 mM $Na_2HPO_4 \cdot 7H_2O$ and pH adjusted to 7.4 ± 0.1 using 1M NaOH and 2M HCl. Custom IR-grade fused silica prisms used as lipid bilayer supports were purchased from Almaz Optics (Marlton, NJ).

Lipid stock solutions of DPPC, DPPC-d62, DSPC, and DSPC-d70 at a concentration of 1 mg/ml in high-performance liquid chromatography (HPLC) grade chloroform were prepared, and a 1 mg/ml solution of C6 NBD-PC in chloroform was used as is from Avanti Polar Lipids. These lipid stock solutions were used to prepare 1 and 3 mol. % C6 NBD-PC in DPPC, DSPC, DPPC-d62, and DSPC-d70 solutions.

Pressure (Π)–area (A) isotherms

Pressure–area isotherms were collected on a Langmuir trough (KSV, Helsinki, Finland). Lipid solutions of 0, 1, and 3 mol. % C6

19 December 2024 21:33:17

Published under an exclusive license by AIP Publishing

NBD-PC in DPPC or DSPC and 100 mol. % C6 NBD-PC in chloroform were deposited at the air–water interface with a PBS solution as the subphase. To ensure solvent evaporation, all lipid monolayers were allowed to sit for 10 min before compression. All monolayers were compressed at a rate of 4 mm/min at a temperature of 20.1 ± 0.2 °C. A 100 point rolling average was applied to each individual isotherm, and an average over three replicate isotherms that did not exceed a deviation of 1 Å^2/molecule throughout was taken for each monolayer system studied.

Planar-supported lipid bilayer (PSLB) preparation

PSLB model membranes were prepared on cleaned IR-grade fused silica support prisms by the Langmuir–Blodgett/Langmuir–Schaefer (LB/LS) method.[31,70] Prior to each use, the prisms were placed in an UV-ozone cleaner (Jetlight Co., Irvine, CA) for 10 min. The prisms were then immersed in piranha solution prepared with three parts 18M sulfuric acid and one part 30% H_2O_2 for a minimum of 60 min. (*Caution: This is a highly corrosive solution and a strong oxidant that reacts violently with organic solvents. Extreme caution must be taken when handling piranha solution.*) Afterward, prisms were rinsed with Nanopure water, dried under a low stream of nitrogen, and treated with argon plasma (Harrick Scientific, Ithaca, NY) for 10 min. Cleaned prisms were submerged in a PBS subphase of the Langmuir trough. The C6 NBD-PC:DPPC and C6 NBD-PC:DSPC mixtures were deposited on the air–water interface of the Langmuir trough and allowed to sit for 10 min to ensure solvent evaporation and equilibrium of the lipids on the surface. After solvent evaporation, monolayers were compressed to a lateral surface pressure of 30 mN/m at a compression rate of 3 mm/min. A lateral surface pressure of 30 mN/m was selected to reflect the approximate pressure observed in solution-phase vesicle systems (30–35 mN/m).[71] Once monolayers reached the desired pressure, the prisms were slowly drawn up out of the subphase to deposit the proximal leaflet by a LB transfer. The trough was then cleaned with isopropyl alcohol, allowed to dry, and rinsed thoroughly with Nanopure water. The second monolayer was then created at the same lateral surface pressure; the prism containing the LB layer was rotated horizontally and then submerged through the second monolayer to form a distal leaflet via a LS transfer. The prisms were then transferred to a custom Teflon flow cell under an aqueous environment. Once in the flow cell, the solution was replaced with a PBS buffer made in D_2O to avoid spectral interference from H_2O in the C–H vibrational mode region.

SFVS experiments

The specific SFVS setup used in these studies has been described in great detail in previous work done by our group,[30,72] and excellent, detailed reviews on the theory of SFVS are also available.[50,51] Before flip-flop kinetic measurements were conducted, a SFVS spectrum was collected from 2750 to 3050 cm^{-1} at 2 cm^{-1} steps and integrated for 10 s at each step to verify the existence of a bilayer on the prism. Flip-flop kinetic experiments were conducted by continuously measuring the CH_3 ν_s mode intensity at 2876 cm^{-1}. Temperature for flip-flop experiments was regulated by a circulating water bath (HAAKE, Phoenix II P1 Circulator, Thermo Fischer Scientific) connected to the flow cell, and the temperature was measured using a type K thermocouple.

SHG experiments

The SHG experimental setup used in these studies has been described in detail in previous work.[62,63,73–75] Briefly, a fundamental 1064 nm source from a Quanta-Ray Pro-Series (Spectra-Physics, Milpitas, CA) was reduced to approximately a 3 mm beam diameter using a Galilean telescope. The intensity of the 1064 nm source was attenuated with a half-wave plate and polarizer. An additional half-wave plate was used to produce mixed s- and p-polarized light, and the resulting mixed polarized beam was brought to the PSLB surface under total internal reflection. A mirror was placed right after the prism, and the beam was redirected back toward the PSLB to produce a counter-propagating SHG (cSHG) geometry. The use of a cSHG configuration was implemented as it has distinct advantages over the more traditional co-propagating geometry. In the counter-propagating setup, the incident photons approach the surface from opposite directions with the use of a mirror, doubling the fundamental optical waves experienced at the surface, which generates a four-time increase in SHG. This is advantageous in PSLB systems where only a small fraction of the lipids are labeled. In addition, the SHG is also produced surface normal due to the conservation of momentum of the photons, eliminating issues of noise generated from the fundamental wave.[63] It is important to note that the beam should never be directly reflected back on itself due to the high likelihood of damaging the laser source. For this reason, the counter-propagating beam is always reflected slightly to the left or right. The detector, a photomultiplier tube (Hamamatsu, Shizuoka, Japan) with 532 nm bandpass filters (Thorlabs, Newton, NJ), was placed surface normal to the PSLB to capture the resulting SHG photons produced from the cSHG setup. The data were acquired using a boxcar integrator (Stanford Research Systems, Sunnyvale, CA) connected to a data acquisition (DAQ) system (National Instruments, Austin, TX), and all data were processed by a custom-made LabVIEW program. Similar to the SFVS experiments, temperature for flip-flop experiments was regulated by a circulating water bath connected to the flow cell and the temperature was measured using a type K thermocouple.

Total internal reflection fluorescence (TIRF) microscopy

TIRF experiments were conducted on a custom modified microscope (Olympus BX40). PSLBs were prepared on the same prisms used for the SFVS and SHG studies. The prism and PSLB were placed on the same flow cell used for the SFVS and SHG experiments. A 405 nm laser diode source was used as the excitation source and was incident at the silica/water surface at an angle of 67°, under total internal reflection, and was modulated at a frequency of 60 Hz using an Ithaco HMS 230 A mechanical chopper (Ithaca, NY). The fluorescence signal was collected using a 3×, long working distance objective with a numerical aperture of 0.08 (Optics for Research, A Division of Thorlabs, Newton, NJ). The fluorescence intensity was measured using a photomultiplier tube with the aid of a lock-in amplifier (Stanford Research Systems). Bandpass filters with a central wavelength of 532 nm (Thorlabs) were used to filter the fluorescence. Data were processed by a DAQ system using

19 December 2024 21:33:17

Published under an exclusive license by AIP Publishing

a custom made LabVIEW program. Briefly, bilayers were made with either a symmetric distribution of 1 mol. % C6 NBD-PC within a DPPC PSLB, and the fluorescence was measured to obtain a maximum fluorescence signal intensity. PBS solutions containing 350 μM or 25 mM dithionite were flowed through the flow cell for the quenching experiments. All dithionite solutions were prepared and used within 2 h of all TIRF experiments. After the experiment was concluded, the detector was closed and 3 ml methanol was flown through the flow cell to destroy the membrane and 3 ml PBS buffer was reintroduced into the cell. The detector was then opened to collect a background signal.

RESULTS AND DISCUSSION

Pressure–area isotherms

The influence of C6 NBD-PC on monolayer packing in both DPPC and DSPC parent lipid matrices was evaluated using pressure–area isotherms (Fig. 2). The mean molecular areas (MMAs) measured at 30 mN/m for monolayers of pure DPPC, 1 mol, 3 mol. %, and pure C6 NBD-PC were 45.2 ± 0.4, 45.2 ± 0.6, 43.1 ± 0.7, and 61.1 ± 0.8 Å^2/molecule, respectively. MMAs for pure DSPC, 1 mol, and 3 mol. % C6 NBD-PC at 30 mN/m were 45.8 ± 0.6, 47.1 ± 0.2, and 50.2 ± 0.7 Å^2/molecule, respectively.

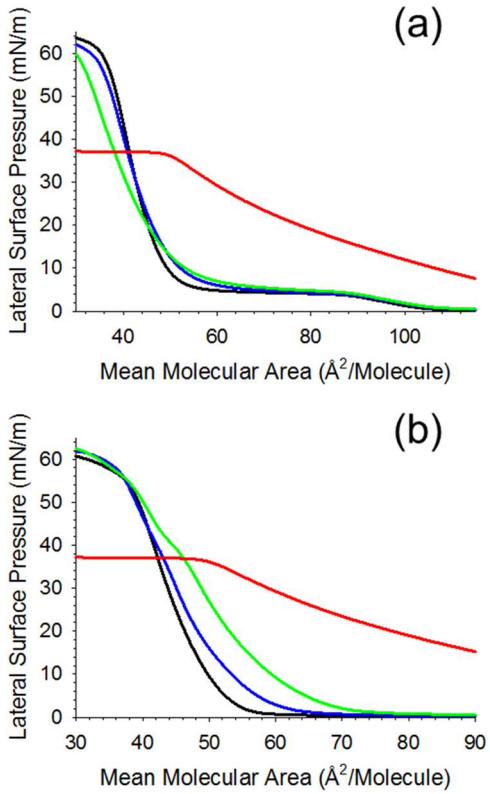

FIG. 2. (a) Pressure–area isotherms of DPPC (black), +1 mol. % C6 NBD-PC (blue), +3 mol. % C6 NBD-PC (green), and pure C6 NBD-PC (red). (b) Pressure–area isotherms of DSPC (black), +1 mol. % C6 NBD-PC (blue), +3 mol. % C6 NBD-PC (green), and pure C6 NBD-PC (red).

The MMAs measured for pure DPPC and DSPC are in good agreement with values previously reported by our group and others.[44,46,76] Isotherms of monolayers containing C6 NBD-PC in DPPC showed that the MMAs at 30 mN/m gradually decreased with the addition of C6 NBD-PC, while a more immediate expansion of the MMA was observed in a DSPC matrix (Fig. 2). Another interesting observation in the DSPC matrix was the emergence of a unique phase transition at ~40 mN/m in the DSPC isotherms, which is not observed in the DPPC isotherms. This abrupt change in slope observed in the DSPC/C6 NBD-PC pressure–area isotherms is associated with a change in compressibility of the membrane and a potential phase separation between DSPC and C6 NBD-PC. This separation of components could have an influence on the energetics associated with mixing and potentially flip-flop measurements (discussed below). This suggests that a mixing behavior between C6 NBD-PC and the two parent lipid matrices is drastically different. Another peculiar observation is the shape of the isotherm of 100% C6 NBD-PC, which has a noticeable deviation from native lipid isotherms such as DPPC and DSPC. The large lateral surface pressures at such high MMAs may be the result of the water soluble NBD moiety moving toward the subphase and the phospholipid headgroups. Another interesting feature of the 100% C6 NBD-PC isotherm is its low collapse pressure at ~37 mN/m. Similar isotherms were collected by Qiao *et al.* for oxidized lipids 1-palmitoyl-2-azelaoyl-sn-*glycero*-3-phosphocholine and 1-palmitoyl-2-(9′-oxo-nonanoyl)-sn-*glycero*-3-phosphocholine, two lipids with shortened *sn*2 chains with a water soluble moiety terminating the chain,[77] similar to C6 NBD-PC, suggesting that water solubility of the chains may be influencing the isotherms drastically with the chains moving from the alkyl chain region in contact with the air toward the headgroups making contact with the subphase. It should be noted that 100% C6 NBD-PC would not be encountered in any reasonable system, but this does illustrate issues that may arise when working with higher concentrations of C6 NBD-PC.

The energetics of C6 NBD-PC mixing with DPPC and DSPC was quantified using the excess free energy of mixing (ΔG^{exc}), using the following expression:

$$\Delta G^{exc} = N \int_0^{\Pi_C} (A_{12} - A_1X_1 - A_2X_2)d\Pi, \tag{16}$$

where N is Avogadro's number, A_{12} is the theoretical MMA of an ideal mixture between the two components, A_1 and A_2 are the MMAs of the first and second components, respectively, X_1 and X_2 are the mole fractions of the first and second components, respectively, and Π_C is the collapse pressure of the monolayer.[78] The excess free energy of mixing as a function of mol. % C6 NBD-PC in both DPPC and DSPC is plotted in Fig. 3. The values for ΔG^{exc} for 1 and 3 mol. % C6 NBD-PC in DPPC were −1 ± 1 and −15 ± 2 kJ/mol, respectively. A ΔG^{exc} of zero is considered ideal mixing with no attractive or repulsive forces between the lipid probe and matrix, suggesting that 1 mol. % C6 NBD-PC in DPPC behaves nearly ideally. At 3 mol. % C6 NBD-PC, the negative ΔG^{exc} indicates that there is favorable mixing between the lipid probe and its matrix due to attractive interactions. The ΔG^{exc} for 1 and 3 mol. % C6 NBD-PC in a DSPC matrix was 7 ± 3 and 24 ± 1 kJ/mol, respectively. The positive values of ΔG^{exc} indicate unfavorable mixing between C6 NBD-PC and the DSPC matrix due to repulsive interactions. This suggests

19 December 2024 21:33:17

Published under an exclusive license by AIP Publishing

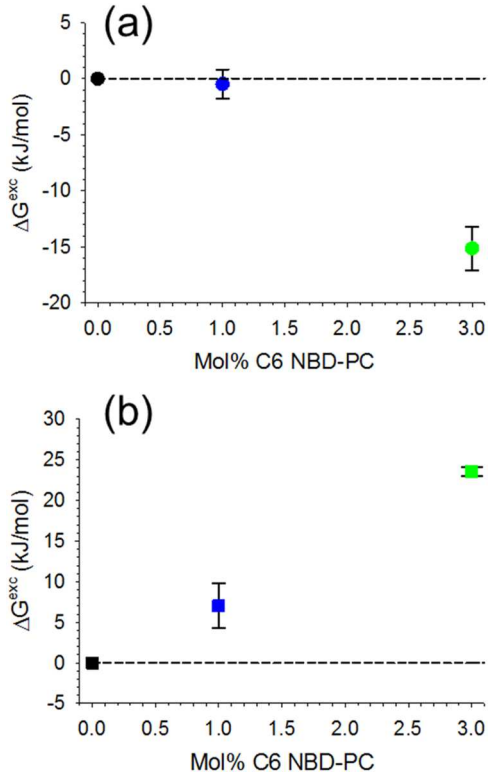

FIG. 3. Excess free energy of mixing as a function of mol. % C6 NBD-PC in (a) DPPC and (b) DSPC. The dashed line represents the excess free energy of mixing of an ideal mixture. Errors in the energy of mixing were propagated from the errors in the MMAs determined from the pressure–area isotherms.

that C6 NBD-PC's impact on its parent lipid matrix varies with the matrix's composition.

C6 NBD-PC lipid chain orientation and ordering

The addition of C6 NBD-PC into the membrane may increase disorder in the membrane's alkyl chains due to the short six-carbon chain containing the NBD label. The "free space" in the hydrocarbon region of the membrane created by the shorter C6 NBD-PC relative to adjacent C16 alkyl chain of the lipid may cause disorder in the chains in the surrounding parent lipid matrix.[79] As a consequence, these disordered alkyl chains could possibly influence the flip-flop of the C6 NBD-PC and potentially the parent lipid matrix if the disorder is significant. There are two methods that can be used to determine the extent of chain ordering of both C6 NBD-PC and the parent lipid matrix. The first is a semi-quantitative approach by examining the relative methyl and methylene signal intensities generated from the alkyl chains in the SFVS spectra, and the second approach is to examine the tilt angle of the terminal methyl group of the acyl chains, as previously described in the Orientation measurements by SFVS section [Eq. (5)].

A well-ordered bilayer would consist of alkyl chains in an *all-trans* conformation. As defects and reorganization of the chains occur within the bilayer, gauche defects are generated, giving rise to a gain in signal at 2849 cm^{-1}, which corresponds to the methylene symmetric stretch (CH_2 ν_s) mode. This mode would not occur in a perfect, *all-trans* system due to a complete cancellation of the CH_2 ν_s transition dipole moments.[37] With this fact, a relative measure of gauche defects within an alkyl chain can be determined using the ratio of the CH_2 ν_s and CH_3 ν_s peak amplitudes found by fitting the SFVS spectra to arrive at a semi-quantitative description of chain ordering.[48,80,81]

The SFVS spectra for 3% C6 NBD-PC in the *ssp* and *sps* polarization states are shown in Fig. 4, and the corresponding methyl tilt angles as well as the CH_2 ν_s/CH_3 ν_s ratios can be found in Table I. The peak assignments for the *ssp* spectra [Figs. 4(a) and 4(b)] are CH_2 ν_s and CH_3 ν_s at 2848 and 2876 cm^{-1}, respectively. Other peaks include a small shoulder peak at 2905 cm^{-1}, which has been attributed to the CH_2 Fermi resonance (CH_2 FR), and a peak centered near 2950 cm^{-1}, which is a combination of the CH_3 Fermi resonance (CH_3 FR) at 2938 cm^{-1} and the CH_3 antisymmetric stretch (CH_3 ν_{as}) at 2960 cm^{-1}.[30,81–83] The peak assignments for the *sps* spectra [Figs. 4(c) and 4(d)] include a dominant peak at 2960 cm^{-1} corresponding to the CH_3 ν_{as} mode and weaker modes at 2852, 2890, and 2912 cm^{-1} that are assigned to the CH_2 ν_s mode, a C–H resonance from the glycerol group, and the methylene antisymmetric stretch (CH_2 ν_{as}), respectively.[31] Tilt angle measurements for 1% C6 NBD-PC were not possible due to inadequate signal-to-noise in the *sps* polarization spectra.

When examining the CH_2 ν_s/CH_3 ν_s ratio for 3 mol. % C6 NBD-PC in the two matrices, it can be seen that the labeled lipid has drastically different gauche content, with the ratio being 0.03 ± 0.04 in DPPC and 0.4 ± 0.2 in DSPC. The errors were determined from three replicate measurements. This increased gauche content is coupled with an increase in the tilt angle of the terminal methyl group of C6 NBD-PC in the DSPC matrix vs the DPPC matrix (Table I). The methyl tilt angles for C6 NBD-PC in DPPC and DSPC were found to be 20° ± 4° in DPPC and 27° ± 2°, respectively. The tilt angles found for C6 NBD-PC in the DPPC matrix agree well with tilts measured for native DSPC.[31] The similar CH_2 ν_s/CH_3 ν_s ratios as well as similar tilt angles for 3% C6 NBD-PC in DPPC suggest that the labeled lipid is well ordered within the chain matched membrane, even with the shortened chain of C6 NBD-PC. C6 NBD-PC in DSPC shows a much higher CH_2 ν_s/CH_3 ν_s ratio as well as a larger tilt angle, suggesting that there is disorder in the alkyl chain of C6 NBD-PC in these DSPC matrices. Because of the increased gauche content, the appropriateness of the delta function distribution assumption used for tilt angle calculations is reduced for the DSPC matrix but still illustrates that the C6 NBD-PC alkyl chains are more disordered within the DSPC matrix when compared to the DPPC matrix. This is likely due to the chain mismatched nature of C6 NBD-PC in the DSPC matrix. Another interesting observation is the change of peak phase for C6 NBD-PC in the different matrices within the *ssp* spectra [Figs. 4(a) and 4(b)]. In the DPPC matrix, the phase of the CH_2 FR and CH_3 ν_{as} modes is positive and negative, respectively, which is the phase observed in native lipid spectra.[31,84] In contrast, the C6 NBD-PC in the DSPC matrix has a negative CH_2 FR and a positive CH_3 ν_{as}. The peaks become negative when destructive interference with the mode of an adjoining peak occurs, suggesting further that the C6 NBD-PC's orientation in DSPC differs significantly from that of the native lipids.

19 December 2024 21:33:17

Published under an exclusive license by AIP Publishing

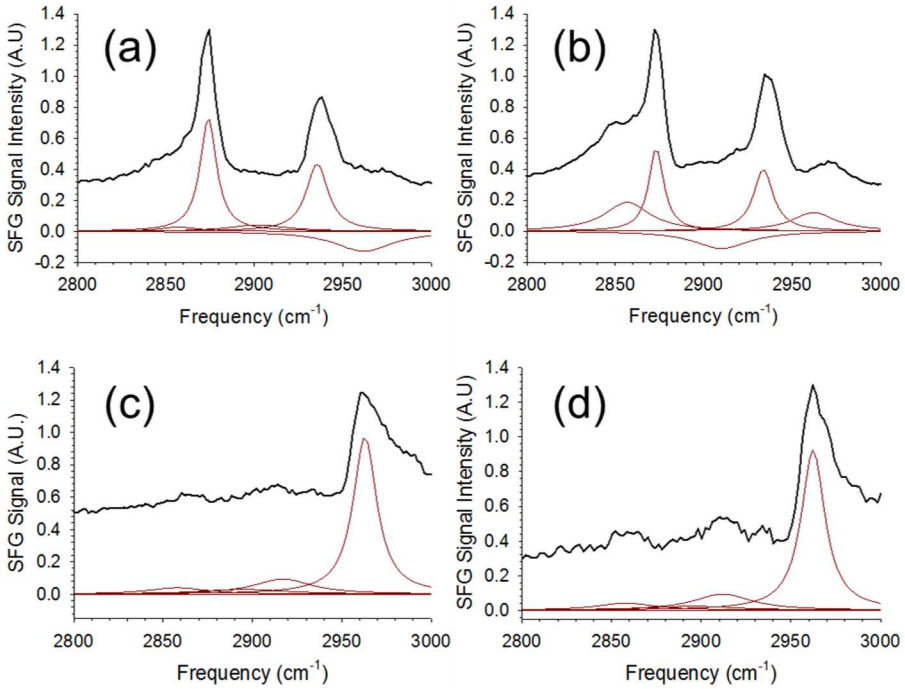

FIG. 4. SFVS spectra of 3 mol. % C6 NBD-PC in DPPC-d62 for (a) *ssp* polarization and (c) *sps* polarization and in DSPC-d70 for (b) *ssp* polarization and (d) *sps* polarization. The fits to the spectra are shown in red and are offset for clarity.

It has been well documented that chain length heterogeneities lead to interdigitation that can increase disorder within the alkyl chains of lipid bilayers.[79,85,86] In the C6 NBD-PC/DSPC system, the difference in the 18-carbon chain DSPC and the 16-carbon and shortened 6-carbon chains of C6 NBD-PC must exist, creating a significant amount of interdigitation to cause an increase in gauche isomerization and disorder within the membrane. It should be noted that there was no statistically significant increase in the gauche content of DSPC at 3 mol. % C6 NBD-PC (supplementary material, Fig. S1), which is most likely due to the total number of DSPC lipids being probed relative to the number of C6 NBD-PC lipids. This suggests that there is a local disorder involving a small population of DSPC interdigitating with the C6 NBD-PC lipids, but the major population of DSPC is well ordered. It is important to note that drastically different results in the chain ordering were observed between DPPC and DSPC, which is a simple chain length substitution, and it must be stressed that the parent lipid matrix composition can play a large role in the labeled lipid's behavior.

TABLE I. CH_3 tilt angle, alkyl chain tilt angle, and CH_2/CH_3 ratios for 3% C6 NBD-PC in DPPC-d62 and DSPC-d70 lipid matrices.

Lipid matrix	$-CH_3$ tilt	CH_2 ν_s/CH_3 ν_s
DPPC-d62	$20^\circ \pm 4^\circ$	0.03 ± 0.04
DSPC-d70	$27^\circ \pm 2^\circ$	0.4 ± 0.2

C6 NBD-PC flip-flop kinetics and thermodynamics

C6 NBD-PC flip-flop kinetics

The flip-flop kinetics of C6 NBD-PC were measured and showed deviations from those of the native phospholipids. Bilayers used to study C6 NBD-PC flip-flop were generated with a proximal leaflet composed entirely of DPPC-d62 or DSPC-d70 and a distal leaflet composed of DPPC-d62 or DSPC-d70 with 1 or 3 mol. % C6 NBD-PC. It should be noted that once complete mixing occurs, and the labeled lipid is equally distributed between the two leaflets that the 1 and 3 mol. % C6 NBD-PC membranes contain an overall 0.5 and 1.5 mol. %, respectively. These bilayers allow for a sum-frequency response that can only arise from the proteated C6 NBD-PC lipids within the bilayer. Bilayers with C6 NBD-PC in the proximal leaflet were tested to ensure that the labeled lipid did not have an affinity to the silica substrate. There were no differences in the rate of flip-flop for C6 NBD-PC between the proximal and distal leaflets.

The rate of C6 NBD-PC flip-flop was measured over a range of temperatures at 1 and 3 mol. % in both DPPC-d62 and DSPC-d70 parent lipid matrices. The decays associated with flip-flop were fit to Eq. (10), and the half-lives were calculated using Eq. (11). The raw decay data (supplementary material, Figs. S2–S5) for C6 NBD-PC show similar single exponential decays that have been measured previously for flip-flop of unlabeled lipids. Table II lists the associated rates and half-lives for DPPC and DSPC measured at several temperatures as well as C6 NBD-PC flip-flop at 1 and 3 mol. % in both DPPC-d62 and DSPC-d70 systems.

19 December 2024 21:33:17

Published under an exclusive license by AIP Publishing

TABLE II. Flip-flop rates and half-lives for DPPC, DSPC, and 1 and 3 mol. % C6 NBD-PC in DPPC and DSPC bilayers as a function of temperature. Flip-flop rates for pure DPPC and DSPC are from Liu and Conboy.[30]

DPPC	[C6 NBD-PC] (mol. %)	Temperature (°C)	Rate ($k \times 10^5$) (s^{-1})	Half-life ($t_{1/2}$) (min)
	0%	27.7 ± 0.1	3.95 ± 0.02	146 ± 1
		29.7 ± 0.1	8.04 ± 0.02	71.8 ± 0.2
		30.5 ± 0.1	11.6 ± 0.03	49.8 ± 0.1
		31.5 ± 0.1	15.5 ± 0.05	37.3 ± 0.1
		32.3 ± 0.1	18.9 ± 0.07	30.5 ± 0.1
		36.0 ± 0.1	42.2 ± 0.29	13.7 ± 0.1
		36.6 ± 0.1	62.8 ± 0.51	9.20 ± 0.07
	1%	22.5 ± 0.1	1.92 ± 0.05	301 ± 8
		24.0 ± 0.1	3.95 ± 0.08	188 ± 5
		25.5 ± 0.1	5.19 ± 0.07	111 ± 1
		27.0 ± 0.1	6.74 ± 0.13	86 ± 2
		30.1 ± 0.1	15.9 ± 0.3	36.3 ± 0.6
		31.4 ± 0.2	20.7 ± 0.3	28.0 ± 0.4
	3%	21.6 ± 0.1	2.00 ± 0.02	288 ± 3
		22.7 ± 0.2	3.71 ± 0.17	156 ± 8
		25.0 ± 0.1	6.16 ± 0.12	94 ± 2
		28.0 ± 0.1	15.1 ± 0.36	38 ± 1
		31.5 ± 0.1	40.5 ± 1.55	14 ± 1
DSPC				
	0%	41.7 ± 0.3	1.85 ± 0.01	312 ± 2
		44.5 ± 0.3	3.60 ± 0.01	160 ± 1
		45.7 ± 0.3	4.67 ± 0.02	124 ± 1
		46.3 ± 0.4	6.72 ± 0.01	86.0 ± 0.1
		49.2 ± 0.2	8.35 ± 0.02	69.2 ± 0.2
		50.3 ± 0.1	15.2 ± 0.06	38.1 ± 0.2
		51.3 ± 0.2	22.3 ± 0.07	25.9 ± 0.1
	1%	30.1 ± 0.1	1.28 ± 0.01	452 ± 4
		32.5 ± 0.1	3.36 ± 0.08	172 ± 4
		32.6 ± 0.1	5.09 ± 0.19	114 ± 4
		34.5 ± 0.2	11.0 ± 0.43	53 ± 2
		34.9 ± 0.1	17.9 ± 0.94	32 ± 2
	3%	30.9 ± 0.1	2.18 ± 0.03	265 ± 4
		32.0 ± 0.1	4.37 ± 0.05	132 ± 2
		35.4 ± 0.1	15.5 ± 1.65	37 ± 4
		35.5 ± 0.2	18.6 ± 0.70	31 ± 1
		36.6 ± 0.2	28.8 ± 1.75	20 ± 1

The SFVS results reveal that C6 NBD-PC exhibits a unique flip-flop behavior compared to its surrounding lipid matrix. It can be seen that the flip-flop rate of C6 NBD-PC differs from both the flip-flop rates of pure DPPC and pure DSPC membranes. In the chain matched DPPC-d62 matrix, the flip-flop rates of C6 NBD-PC are slightly faster when compared to DPPC flip-flop rates. For example, the half-life for flip-flop of DPPC, 1 mol. %, and 3 mol. % C6 NBD-PC in DPPC-d62 at 31.5 °C was 37.3 ± 0.1, 28.0 ± 0.4, and 14 ± 1 min, respectively. C6 NBD-PC had consistently faster flip-flop rates at all temperatures tested in DPPC, which can be seen in Table II. When comparing the activation thermodynamics of DPPC and C6 NBD-PC in a DPPC-d62 matrix, it was found that there was no statistical difference in the activation enthalpy or entropy when comparing the matrix lipid DPPC to C6 NBD-PC. The Gibbs plot for this system and all other systems can be found in the supplementary material (Fig. S6). The activation enthalpies for DPPC, 1, and 3 mol. % C6 NBD-PC were 221 ± 12, 196 ± 7, and 216 ± 11 kJ/mol, respectively, and the activation entropies were 407 ± 41, 328 ± 23, and 398 ± 35 J/mol K, respectively. However, in the chain mismatched system, a more drastic difference between C6 NBD-PC and DSPC flip-flop rates and dynamics was observed. C6 NBD-PC flip-flop rates in DSPC-d70 were too fast to measure at the temperatures conducted for DSPC (Table II). If the C6 NBD-PC data are extrapolated to 46.3 °C, the half-lives for C6 NBD-PC at 1 and 3 mol. % are 8 and 27 s, respectively. The corresponding DSPC half-life at 46.3 °C is 86.0 ± 0.1 min, remarkably slower than the C6 NBD-PC. This large discrepancy between the flip-flop rates between C6 NBD-PC and DSPC is unsurprising, as it has been shown previously that the activation free energy for flip-flop increases ~14 kJ/mol per two carbon addition to the alkyl chain of saturated lipids.[87] Since the C6 NBD-PC is chain matched with DPPC (C-16), it would be expected that C6 NBD-PC would behave more closely to DPPC than DSPC. Using Eq. (12) and the extrapolated rates for C6 NBD-PC at 46.3 °C, the free energy of activation for DSPC, 1, and 3 mol. % C6 NBD-PC in DSPC-d70 are 104, 87, and 90 kJ/mol, respectively. This result is interesting as it shows the approximate 14 kJ/mol increase in the activation energy one would expect between DPPC and DSPC. When examining the activation thermodynamics for C6 NBD-PC in DSPC-d70, a drastic change was observed. The activation enthalpy for DSPC, 1, and 3 mol. % C6 NBD-PC was 204 ± 18, 410 ± 40, and 341 ± 17 kJ/mol, respectively, and the activation entropy was 313 ± 57, 1013 ± 130, and 789 ± 56 J/mol K, respectively. These results suggest that C6 NBD-PC mimics the chain matched DPPC system better in terms of both its rates and thermodynamics when compared to the chain mismatched DSPC system, where severe differences in flip-flop rates and thermodynamics are observed. The large deviations in the flip-flop rates and activation thermodynamics, the activation entropy in particular, for C6 NBD-PC in the DSPC system may be attributed to the chain mismatching, causing an increase in chain disorder and gauche content of C6 NBD-PC, which was observed in the SFVS analysis of the gauche content and acyl chain tilt discussed above (Table I). It should be noted that while C6 NBD-PC does not mimic DPPC perfectly, the rates obtained show that C6 NBD-PC is a significantly better reporter than other probes such as spin labeled TEMPO-DPPC and other fluorescently labeled lipids such as pyrene labeled lipids,[12,88] but its inability to faithfully mimic the DSPC system should not be ignored when interpreting C6 NBD-PC's ability to report flip-flop kinetics. The sum of these results indicates that the matrix plays a significant role in how C6 NBD-PC behaves both in orientation and in its kinetics and thermodynamics.

When comparing the C6 NBD-PC data obtained by SFVS to that measured in previous fluorescence studies, there are discrepancies in the rates obtained. When looking at 1 mol. % C6 NBD-PC in DPPC small unilamellar vesicles (SUVs), John *et al.* did not observe any noticeable change in the fluorescence intensity after the initial

19 December 2024 21:33:17

Published under an exclusive license by AIP Publishing

quenching by dithionate at 30 °C and concluded that flip-flop did not occur, arguing that flip-flop is a slow process in the gel state.[17] Quenching, and by extension flip-flop, was observed in SUVs only at the phase transition temperature (41 °C) of DPPC ($t_{1/2}$ = ~9 min) and above the phase transition temperature ($t_{1/2}$ = ~40 min) at 50 °C. Our experiments show that flip-flop does occur at 30 °C in a DPPC matrix, with a half-life of 36.3 ± 0.6 min at 30.1 ± 0.1 °C for DPPC PSLBs containing 1 mol. % C6 NBD-PC. Extrapolation of the SFVS data to 41 °C gives a flip-flop rate of ~2 min for 1% C6 NBD-PC in a DPPC matrix, slightly faster than what was measured by fluorescence but not on a dissimilar timescale.

The major differences between the fluorescence studies and the current study that could contribute to the discrepancies seen in the measured rates of flip-flop are the use of different membrane models, SUVs vs PSLBs, and the absence of dithionite in the SFVS studies as quenching of the fluorophore was not necessary. To test whether dithionite could potentially be altering the flip-flop kinetics of C6 NBD-PC, SFVS flip-flop decays were conducted on 1 mol. % C6 NBD-PC in DPPC-d62 PSLBs in the presence of PBS buffer with the addition of 350 μM dithionite. 350 μM dithionite was chosen to reflect the approximate 1:360 lipid:dithionite mole ratio used in the fluorescence study by John *et al.*[17] In addition to dithionite's influence on C6 NBD-PC, DPPC flip-flop decays were also conducted in the presence of 350 μM dithionite to determine whether the quenching reagent had an influence on native lipid flip-flop. This was done by creating the PSLB in a PBS buffer solution free of dithionite and then flowing a D_2O buffer solution containing 350 μM dithionite through the system. The raw SFVS decay data of these bilayers can be found in the supplementary material (Figs. S7 and S8). An Eyring plot showing the rate of flip-flop of DPPC and C6 NBD-PC in the absence (black and blue circles) and presence (gray and cyan triangles) of 350 μM dithionite can be found in Fig. 5. The DPPC flip-flop half-lives in the presence of dithionite at 29.4 ± 0.2, 33.0 ± 0.3, and 34.1 ± 0.1 °C were 65.3 ± 0.7, 27.9 ± 0.9, and 14.7 ± 0.3 min, respectively, all within the 95% confidence interval of the SFVS measurements in the absence of dithionite. The 1% C6 NBD-PC measurement at 30.6 ± 0.1 °C had a half-life of 36 ± 1 min, which was also within the confidence interval of SFVS measurements that lacked dithionite. It can be concluded that dithionite does not alter the flip-flop rates of C6 NBD-PC nor DPPC, suggesting that dithionite has little influence on lipid flip-flop kinetics at the concentration tested.

It can be seen that even in the presence of 350 μM dithionite, C6 NBD-PC has a flip-flop rate of 36 ± 1 min at 30.6 °C, a rate that should have been detectable by fluorescence quenching. This suggests that the presence of dithionite alone is not capable of altering flip-flop kinetics in a meaningful way. However, these SFVS results alone do not exclude the possibility that dithionite is incapable of permeating the bilayer's hydrophobic core to quench the tail labeled NBD at this temperature and additional experimentation would be needed to verify this claim (see below). This is especially true at 30 °C where DPPC membranes are in the gel phase, limiting permeation of dithionite to reach the NBD moiety.[89,90] This creates a scenario in which it appears as if the NBD is not translocating when in fact it is the reporter NBD that is not accessible to dithionite.

In order to test the ability of dithionite to quench C6 NBD-PC in gel state DPPC membranes, TIRF microscopy was used. In the following experiments, 1 mol. % C6 NBD-PC in a DPPC matrix was exposed to 350 μM dithionite at room temperature to determine if quenching of the NBD occurs. The TIRF quenching experiments can be found in Fig. 6, where it can be seen that quenching did not occur in the presence of 350 μM dithionite with an average fluorescence intensity after dithionite injection being 97% ± 1% of the

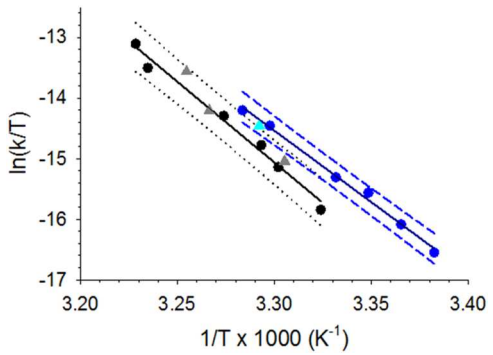

FIG. 5. Eyring plot of DPPC (black circles) and 1 mol. % C6 NBD-PC (blue) at 0 μM dithionite and DPPC (gray triangles) and 1 mol. % C6 NBD-PC (cyan triangle) in the presence of 350 μM dithionite. The black dotted lines and blue dashed lines indicate the 95% confidence interval for DPPC and C6 NBD-PC, respectively.

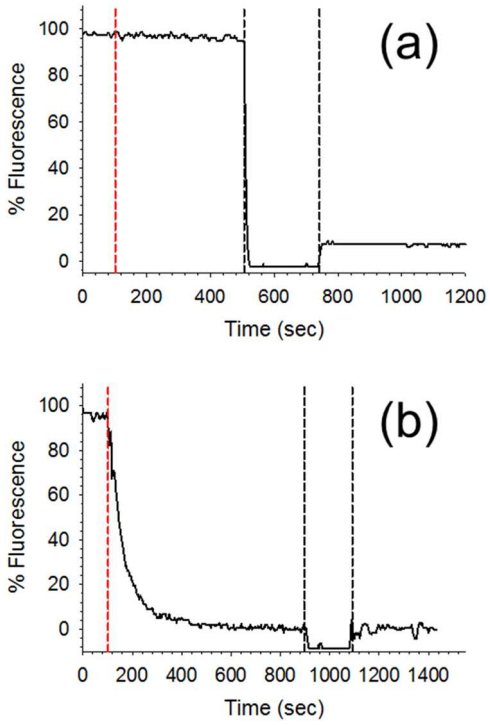

FIG. 6. TIRF fluorescence experiments to determine NBD quenching for 1 mol. % C6 NBD-PC in a DPPC PSLB upon the addition of (a) 350 μM and (b) 25 mM dithionite. The red dashed line indicates the time in which dithionite was injected into the system (after 100 s), and the black dashed lines indicate when the detector was closed, the membrane was destroyed with methanol, and buffer was reintroduced into the system to collect a baseline.

19 December 2024 21:33:17

Published under an exclusive license by AIP Publishing

initial fluorescence intensity prior to the introduction of dithionite. This is in agreement with dithionite's partition coefficient,[91] suggesting that its presence within the hydrophobic core is unlikely. It has been shown, however, that significant excess of dithionite is more readily able to penetrate the membrane.[92] To verify that the TIRF instrument was capable of measuring NBD quenching by dithionite, a 1 mol. % C6 NBD-PC + DPPC bilayer was incubated with 25 mM dithionite [Fig. 6(b)], which shows a rapid quenching of C6 NBD-PC. These results suggest that at 350 μM dithionite, an approximate 1:360 lipid:dithionite mole ratio, or a 1:36 000 NBD:dithionite mole ratio when one considers that only 1% of lipids contain the NBD moiety, quenching does not occur in the gel phase, at least in PSLB models.

This lack of quenching is in contradiction to John *et al.* who used a similar lipid:dithionite ratio and observed complete quenching of the outer leaflet at 10 °C within 10 minutes. However, it should be noted that the vesicle solution was initially injected with dithionite solution at an elevated temperature and then rapidly cooled to 10 °C to mitigate flip-flop. It is peculiar that quenching can occur at all in these tail labeled lipids, given that the NBD moiety is within the hydrophobic core of the membrane, which should presumably restrict the hydrophilic dithionite from readily reacting with NBD. As previously mentioned, it is presumed that dithionite can quench the outer leaflet of vesicle systems but does not have the ability to quench the inner leaflet, suggesting that dithionite partially permeates through the membrane to facilitate the reduction reaction.[17] This partial permeation is not chemically intuitive, as one would expect if the dithionite has access to the outer leaflet's NBD within the hydrophobic space, the dithionite's proximity to the inner leaflet's NBD is not unreasonably far, especially in the gel state where the NBD moiety is buried in the hydrophobic core. However, this is not true in the liquid-crystalline phase where NBD has a propensity to loop up toward the hydrophilic headgroup. It has been observed through red edge excitation shift (REES) experiments that the NBD moiety of a variety of tail labeled NBD lipids have the ability to loop up from the hydrophobic core toward the hydrophilic head group changing its dipole orientation, but only in fluid phase membranes where movement of the acyl chains is not restricted.[89,90] It is reasonable then that the initial reduction of NBD in the DPPC SUVs at 41 and 50 °C observed by John *et al.* readily occurs as the NBD moiety is already looped, allowing for immediate access by dithionite to facilitate the reduction of the outer leaflet and subsequent flip-flop can follow, which was shown to be on the order of minutes, similar to SFVS measurements. This would also explain why no additional quenching was observed at 30 °C in the SUV system as the NBD would not be looped and is within the hydrophobic core, limiting dithionite's access to the NBD moiety.

Other factors that could explain the initial quenching in vesicle systems are the fusion of individual vesicles and the permeability of the vesicles. It is possible that vesicle fusion could play a role in partial quenching of these vesicle systems; however, John *et al.* claimed that no such fusion was occurring. This was tested by incubating their vesicles at 41 °C for 2 h and only examined the outer leaflet population change from 65% to 62%, indicating a diameter increase of approximately a few nanometers.[17] Dynamic light scattering was not used to verify that vesicle fusion was not occurring in the system, so the contribution of vesicle fusion to the observed quenching cannot be completely ruled out. Another factor that can contribute to quenching that was not discussed in the fluorescence study by John *et al.* is the influence dithionite permeation can have on the flip-flop rates obtained by fluorescence quenching. It has been previously shown that the rate of dithionite permeability is greatest at the phase transition temperature, where the highest level of disorder occurs in the membrane.[93] Langner and Hui showed for head labeled 1,2-dipalmitoyl-sn-*glycero*-3-phosphoethanolamine-*N*-(7-nitro-2-1,3-benzoxadiazol-4-yl) (NBD-PE) in multilayer 1,2-dimyristoyl-sn-*glycero*-3-phosphocholine (DMPC) vesicles that the quenching by dithionite was greatest at the phase transition of DMPC (24 °C) and a subsequent decrease in the rate of quenching was observed past the phase transition (37 °C), resembling the rates observed below the phase transition temperature (17 °C).[93] Langner and Hui attributed this observation purely to the permeability of the dithionite through the vesicles and claimed that molecular packing defects, which are maximized at the gel–fluid phase transition, increase this permeability. The results of this study are important as the use of a head labeled NBD-PE probe removed the looping aspect. It should also be noted that there was no mention of the quenching in this study being attributed to lipid flip-flop. To strengthen the argument that packing defects dictate dithionite diffusion through the membrane, Moreno *et al.* attempted to decouple the rates of translocation and dithionite permeability and showed that dithionite permeability was fastest in the liquid disordered phase of 1-palmitoyl-2-oleoyl-*glycero*-3-phosphocholine (POPC) large unilamellar vesicles (LUVs) and the permeability decreased in the liquid ordered state for both tail labeled and head labeled NBD lipids.[94] These issues highlight the difficulties in interpreting flip-flop kinetics in vesicle systems using fluorescence probes as other factors such as looping, vesicle fusion, and reducing agent permeation cannot be ignored and all play a role in potentially altering or leading to a misinterpretation of the kinetics observed. This shows why SFVS is an attractive method to measure flip-flop when compared to fluorescence quenching experiments as it reliably measures flip-flop only and does not rely on the quenching of a label, which can occur through a variety of processes such as flip-flop, looping, vesicle fusion, or reducing agent permeability.

Measuring C6 NBD-PC flip-flop via SHG

In addition to the issues discussed above, it is possible that the discrepancies between the fluorescence and SFVS results also could arise if the movement of the NBD moiety differs from that of the adjacent alkyl chain measured using SFVS. To better understand the movement of the NBD moiety, the flip-flop rates of 3 mol. % C6 NBD-PC in DPPC were measured by SHG, which probes the transition dipole of the NBD label.

The use of SHG to probe kinetic events such as molecular transport across lipid membranes has been established in the literature by Kim, Eisenthal, and Dai.[64–69] For example, Eisenthal's group has shown that the adsorption and subsequent transport kinetics of the SHG-active cationic organic dye malachite green (MG) across large unilamellar vesicles (LUVs) composed of POPC and 1-palmitoyl-2-oleoyl-sn-*glycero*-3-phospho-(1′-rac-glycerol) (POPG) could be measured via SHG.[65] In their experiment, MG was introduced to the outside of POPC/POPG LUVs and a subsequent adsorption of the MG to the surface of the liposomes caused an initial SHG signal increase due to the adsorption of MG on the outer leaflet of the

19 December 2024 21:33:17

Published under an exclusive license by AIP Publishing

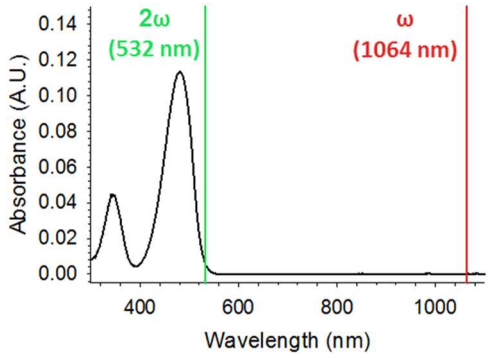

FIG. 7. UV–visible spectrum of 5.4 μM C6 NBD-PC.

vesicle. As transport of MG through the membrane occurs, a resulting decrease in the SHG signal was measured due to a cancellation of the electronic transitions of MG in the inner and outer leaflets of the LUVs. This gain in symmetry and a subsequent decrease in the SHG signal intensity are reminiscent of sum-frequency flip-flop signal decay, which is governed by Eqs. (9) and (10), with the main difference being the probing of electronic transitions vs vibrational modes. This suggests that flip-flop is also measurable via SHG as long as there is an asymmetric distribution of transitional dipole moments as was the case for the initial asymmetric distribution of MG. This was tested by generating an asymmetric PSLBs containing 3 mol. % C6 NBD-PC in one leaflet and measuring the decay associated with the flip-flop of C6 NBD-PC in a DPPC matrix. A fundamental source of 1064 nm was used to produce 532 nm SHG, which is near resonance with C6 NBD-PC, which can be seen in the UV–visible spectrum collected for 5.4 μM C6 NBD-PC in Fig. 7. The flip-flop measurements were conducted similar to SFVS, and Fig. 8 shows an Eyring plot containing the flip-flop rates for DPPC obtained by SFVS and 3 mol. % C6 NBD-PC measured by SHG. The raw SHG decay plots can be found in the supplementary material (Fig. S9). It can be seen in Fig. 8 that there is no statistical difference in the decay rates for 3% C6 NBD-PC measured by SFVS and SHG. This suggests that there are no discrepancies between using

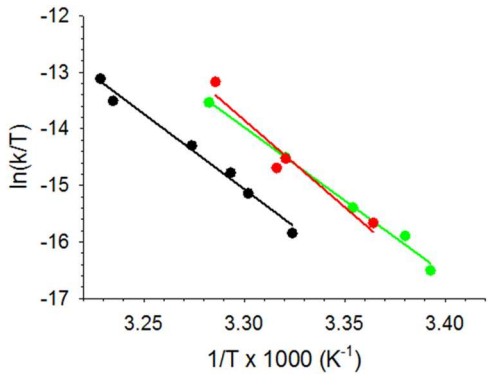

FIG. 8. Sample flip-flop decays for 3 mol. % C6 NBD-PC at 28.0 °C using (a) SFVS and (b) 1064 nm cSHG. All decays can be found in the supplementary material.

the methyl group or the NBD moiety of C6 NBD-PC to measure lipid flip-flop, further strengthening the idea that the rates obtained truly reflect the movement of the C6 NBD-PC. Attempts were made to measure 1% C6 NBD-PC via cSHG, but signal-to-noise issues prevented meaningful decays from being collected. If we compare a sample set of decays collected from SFVS and cSHG, which can be found in Fig. 9, it can be seen that SFVS has superior signal-to-noise at 3 mol. % NBD. The decays obtained by SFVS [Fig. 9(a)] and cSHG [Fig. 9(b)] were both conducted at 28.0 °C and have a flip-flop half-life of 38 ± 1 and 39 ± 3 min, respectively, showing that even with the reduced signal-to-noise, the cSHG data are within error of the SFVS data. The reason for this issue is most likely due to SFVS being on the exact vibrational frequency required, while the SHG fundamental frequency, and by extension the SHG, used in these experiments is off of the max resonance. It can be seen in Fig. 7 that the SHG at 532 nm is just on the edge of the max resonance of C6 NBD-PC, which limits the achievable SHG signal intensity. If one has the ability to shift the fundamental frequency to optimize the SHG toward the max absorbance, a substantial increase in SHG would be possible. It is important to note that at 3 mol. % C6 NBD-PC, only ~20 pmol is expected on the surface of the prisms used as a solid support and illustrates, even when off max resonance, how impressive SHG can be in probing these kinetics.

As a final note, these SHG results also suggest that the deuteration of the PSLB and D_2O required for SFVS measurements has no major influence on the flip-flop rates of C6 NBD-PC as the

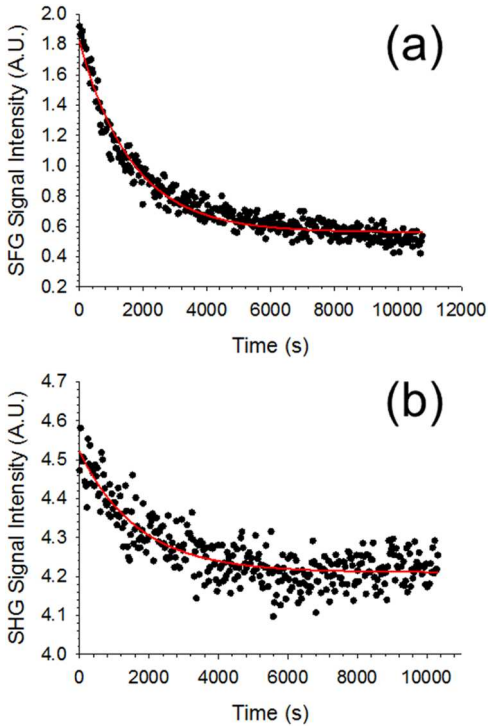

FIG. 9. Eyring plot of the rates of flip-flop for DPPC (black circles), 3 mol. % C6 NBD-PC measured by SFVS (green circles), and 3 mol. % C6 NBD-PC measured by SHG (red circles).

19 December 2024 21:33:17

Published under an exclusive license by AIP Publishing

SFVS PSLBs contained a fully DPPC-d62 matrix, while the SHG experiments were conducted in a DPPC matrix. To the best of our knowledge, this is the first instance of SHG being used to measure phospholipid flip-flop, specifically. This could have important implications in systems where SFVS is not possible due to the deuteration of lipids being inconvenient or impossible. Future work will be done to optimize and enhance the SHG signal to probe membranes at even lower concentrations of biologically relevant material.

Influence of C6 NBD-PC on parent matrix flip-flop kinetics

Small quantities of C6 NBD-PC have been shown to perturb the lipid matrix in vesicle systems, broadening and shifting the phase transition temperatures.[29] To test the influence C6 NBD-PC has on the flip-flop kinetics of the lipid matrix surrounding it, the flip-flop of DPPC and DSPC in the presence of 1 and 3 mol. % C6 NBD-PC was measured and compared to the native rates of flip-flop. Bilayers used in these studies were created with a proximal leaflet composed of DPPC-d62 or DSPC-d70 and a distal leaflet of DPPC or DSPC containing 1 or 3 mol. % C6 NBD-PC. The flip-flop of DPPC and DSPC was measured over a range of temperatures and fit to Eqs. (10) and (11) to determine the rate and half-lives for flip-flop, respectively. The raw decay data can be found in Figs. S10–S13 of the supplementary material, as well as the tabulated rates for parent lipid flip-flop and the corresponding half-lives can be found in Table SI. It was observed that the flip-flop rates for DPPC and DSPC are essentially unperturbed at 1 mol. % C6 NBD-PC, but the rate of flip-flop does increase in the presence of 3 mol. % C6 NBD-PC. For example, DPPC half-lives at 0 and 3 mol. % C6 NBD-PC were 71.8 ± 0.2 and 44.0 ± 0.3 min at 29.7 and 29.3 °C, respectively, and the half-lives of DSPC at 0 and 3 mol. % C6 NBD-PC at 49.1 °C were 69.2 ± 0.2 and 23 ± 1 min, respectively. This suggests that larger concentrations of C6 NBD-PC can begin to affect the surrounding lipid matrix. The Gibbs plots for the parent lipid matrix can be found in the supplementary material (Fig. S6). The activation enthalpy for DPPC, DPPC with 1 mol. % C6 NBD-PC present, and DPPC with 3 mol. % C6 NBD-PC present was 221 ± 12, 215 ± 10, and 257 ± 30 kJ/mol, respectively, while the activation entropy for these systems was 407 ± 41, 385 ± 33, and 533 ± 101 J/mol K, respectively. The activation enthalpy for DSPC, DSPC with 1 mol. %, and DSPC with 3 mol. % C6 NBD-PC was found to be 204 ± 18, 190 ± 42, and 207 ± 40 kJ/mol, respectively, while the activation entropy for these systems was 313 ± 57, 270 ± 131, and 332 ± 126 J/mol K, respectively. In both DPPC and DSPC, the presence of 1 mol. % C6 NBD-PC produces very little difference in the activation barrier to flip-flop, whereas at 3 mol. % C6 NBD-PC, the barrier decreases and the matrix flip-flop rate increases. Interestingly, this lower energy barrier to flip-flop is not reflected in the activation enthalpy or entropy, as the values for 0, 1, and 3 mol. % C6 NBD-PC are all statistically similar. These large errors in the activation enthalpy and entropy have been reported previously by our group and are ultimately a consequence of conducting flip-flop measurements over a limited temperature range.[40] Regardless, this suggests that at 1 mol. %, the lipid matrix is not perturbed significantly, but at higher concentrations, the fluorophore begins to influence the lipid matrix. This may be due to the shift in the phase transition temperature seen in bilayers containing a higher concentration of C6 NBD-PC, essentially accelerating the membrane's kinetics as a whole and is consistent with the behavior observed in the LB isotherms and mixing behavior discussed above.[29]

CONCLUSIONS

Fluorescently labeled lipids have historically been a powerful tool to measure membrane flip-flop kinetics due to their ease of use and the high sensitivity of fluorescence spectroscopy. There are criticisms to be made, however, on how the addition of large fluorescence tags placed on the lipids has the potential to change the flip-flop kinetics, which would limit their use as reporters of native lipid translocation. In addition, the influence labeled lipids may have on the membrane packing and chain ordering cannot be ignored. Arguments have been made that the labeled lipids will mimic the parent lipid behavior if present in the membrane at low enough concentrations. These assumptions were tested in the present study.

The impact of labeled lipids on membrane structure was systematically examined by studying their effect on membrane packing and acyl chain ordering. Analysis of pressure–area isotherms revealed a compressive effect in DPPC monolayers and an expansive effect in DSPC monolayers upon the addition of the labeled lipid. This observation was quantitatively described by a negative Gibbs free energy of mixing for C6 NBD-PC in DPPC, indicating favorable interactions, whereas a positive free energy was observed in DSPC, indicating unfavorable interactions.

Furthermore, the conformational ordering of C6 NBD-PC acyl chains was investigated by evaluating the gauche content using the methylene-to-methyl ratio and by determining the tilt angle of the terminal methyl group on the alkyl chain. It was observed that C6 NBD-PC in DPPC bilayers maintained the gauche content and tilt angles comparable to those of the DPPC matrix lipids, suggesting that the labeled lipid adapts its acyl chain conformation well in a matched chain length environment. In contrast, C6 NBD-PC exhibited significantly increased gauche content and larger tilt angles in DSPC bilayers, indicating a higher disorder in its acyl chain, likely due to the mismatch in chain length between C6 NBD-PC and DSPC, which allows for more conformational freedom. This study further demonstrated that the gauche content of the native lipid matrix remained largely unaffected at 3 mol. % inclusion of C6 NBD-PC for both DPPC and DSPC systems.

Kinetic and thermodynamic analyses of C6 NBD-PC flip-flop were performed using SFVS at concentrations of 1 and 3 mol. %, in both DPPC and DSPC matrices. Results showed that C6 NBD-PC exhibited faster flip-flop rates than the parent lipids, with notably faster rates in DSPC, indicating that the labeled lipid does not mimic the behavior of the native matrix effectively.

To ensure consistency in the measurement techniques, SHG was employed to specifically probe the NBD moiety. Comparative studies at 3 mol. % C6 NBD-PC in DPPC showed no significant differences between the flip-flop measurements obtained via SFVS and those obtained via SHG probing the NBD moiety. This congruence between the two methods suggests that both methodologies are consistent in their measurements. To our knowledge, this marks the first application of SHG in flip-flop measurements.

The activation thermodynamics of C6 NBD-PC flip-flop in DPPC revealed a slightly lower activation barrier compared to native DPPC. In contrast, the activation thermodynamics in DSPC showed a significant increase, with the activation enthalpy doubling and the

19 December 2024 21:33:17

Published under an exclusive license by AIP Publishing

entropy quadrupling compared to native DSPC. These findings indicate that the lipid matrix significantly influences the kinetics of the labeled lipid, suggesting that more complex systems may further complicate the kinetic interpretations of C6 NBD-PC flip-flop.

Overall, these findings demonstrate that C6 NBD-PC does not mimic the behavior of the parent lipid matrix and that the nature of the lipid matrix in which it is placed (DPPC vs DSPC) can significantly affect the measured flip-flop dynamics of the lipid probe. Therefore, a careful interpretation of kinetic data from labeled lipids is required.

SUPPLEMENTARY MATERIAL

The supplementary material contains the raw SFVS and SHG flip-flop decay data for all experiments conducted in this study, the SFVS spectra for DPPC and DSPC at 0 and 3 mol. % C6 NBD-PC, the Gibbs plots for both C6 NBD-PC and the DPPC/DSPC parent matrices, and a table with calculated flip-flop rates for DPPC and DSPC at 0, 1, and 3 mol. % C6 NBD-PC.

ACKNOWLEDGMENTS

This work was supported by the National Science Foundation (NSF) (Grant No. 1953975). The authors thank Professor Thomas Richmond for gifting the dithionite used within these studies.

AUTHOR DECLARATIONS

Conflict of Interest

The authors have no conflicts to disclose.

Author Contributions

Joshua M. Taylor: Data curation (lead); Formal analysis (equal); Investigation (lead); Methodology (equal); Writing – original draft (lead); Writing – review & editing (equal). **John C. Conboy**: Conceptualization (lead); Data curation (supporting); Formal analysis (equal); Funding acquisition (lead); Investigation (equal); Methodology (equal); Project administration (lead); Resources (lead); Supervision (lead); Writing – original draft (supporting); Writing – review & editing (equal).

DATA AVAILABILITY

The data that support the findings of this study are available from the corresponding author upon reasonable request.

REFERENCES

[1] G. Van Meer, D. R. Voelker, and G. W. Feigenson, Nat. Rev. Mol. Cell Biol. **9**, 112 (2008).
[2] P. F. Devaux, Biochemistry **30**, 1163 (1991).
[3] A. H. Maddy, Biochim. Biophys. Acta, Spec. Sect. Biophys. Subj. **88**, 390 (1964).
[4] M. Ikeda, A. Kihara, and Y. Igarashi, Biol. Pharm. Bull. **29**, 1542 (2006).
[5] J. A. Op den Kamp, Annu. Rev. Biochem. **48**, 47 (1979).
[6] C. F. Higgins, Cell **79**, 393 (1994).
[7] R. J. Clarke, K. R. Hossain, and K. Cao, Biochim. Biophys. Acta, Biomembr. **1862**, 183382 (2020).
[8] P. F. Devaux and A. Herrmann, *Transmembrane Dynamics of Lipids* (John Wiley & Sons, NJ, 2011).
[9] X. Tang, M. S. Halleck, R. A. Schlegel, and P. Williamson, Science **272**, 1495 (1996).
[10] T. Pomorski, R. Lombardi, H. Riezman, P. F. Devaux, G. Van Meer, and J. C. M. Holthuis, Mol. Biol. Cell **14**, 1240 (2003).
[11] C. Chen, M. F. Ingram, P. H. Rosal, and T. R. Graham, J. Cell Biol. **147**, 1223 (1999).
[12] H. M. McConnell and R. D. Kornberg, Biochemistry **10**, 1111 (1971).
[13] P. F. Devaux, P. Fellmann, and P. Hervé, Chem. Phys. Lipids **116**, 115 (2002).
[14] D. W. C. Dekkers, P. Comfurius, A. J. Schroit, E. M. Bevers, and R. F. A. Zwaal, Biochemistry **37**, 14833 (1998).
[15] S. Hrafnsdóttir, J. W. Nichols, and A. K. Menon, Biochemistry **36**, 4969 (1997).
[16] T. Pomorski, P. Müller, B. Zimmermann, K. Burger, P. F. Devaux, A. Herrmann, P. Muller, B. Zimmermann, K. Burger, P. F. Devaux, and A. Herrmann, J. Cell Sci. **109**, 687 (1996).
[17] K. John, S. Schreiber, J. Kubelt, A. Herrmann, and P. Müller, Biophys. J. **83**, 3315 (2002).
[18] M. Nakano, M. Fukuda, T. Kudo, N. Matsuzaki, T. Azuma, K. Sekine, H. Endo, and T. Handa, J. Phys. Chem. B **113**, 6745 (2009).
[19] Y. Gerelli, L. Porcar, L. Lombardi, and G. Fragneto, Langmuir **29**, 12762 (2013).
[20] D. Marquardt, F. A. Heberle, T. Miti, B. Eicher, E. London, J. Katsaras, and G. Pabst, Langmuir **33**, 3731 (2017).
[21] J. Liu and J. C. Conboy, J. Am. Chem. Soc. **126**, 8376 (2004).
[22] A. Chattopadhyay and E. London, Biochim. Biophys. Acta, Biomembr. **938**, 24 (1988).
[23] A. Chattopadhyay, Chem. Phys. Lipids **53**, 1 (1990).
[24] S. Lin and W. S. Struve, Photochem. Photobiol. **54**, 361 (1991).
[25] S. Mukherjee, A. Chattopadhyay, A. Samanta, and T. Soujanya, J. Phys. Chem. **98**, 2809 (1994).
[26] Y. Mely and G. Duportail, *Fluorescent Methods to Study Biological Membranes* (Springer, Berlin, Heidelberg, 2011).
[27] D. Hoekstra, Biochemistry **21**, 2833 (1982).
[28] S. Mazères, V. Schram, J. F. Tocanne, and A. Lopez, Biophys. J. **71**, 327 (1996).
[29] L. M. S. Loura, F. Fernandes, A. C. Fernandes, and J. P. P. Ramalho, Biochim. Biophys. Acta, Biomembr. **1778**, 491 (2008).
[30] J. Liu and J. C. Conboy, Biophys. J. **89**, 2522 (2005).
[31] J. Liu and J. C. Conboy, Langmuir **21**, 9091 (2005).
[32] N. Bloembergen and P. S. Pershan, Phys. Rev. **128**, 606 (1962).
[33] N. Bloembergen, R. K. Chang, and C. H. Lee, Phys. Rev. Lett. **16**, 986 (1966).
[34] C. H. Lee, R. K. Chang, and N. Bloembergen, Phys. Rev. Lett. **18**, 167 (1967).
[35] N. Bloembergen, R. K. Chang, S. S. Jha, and C. H. Lee, Phys. Rev. **174**, 813 (1968).
[36] Y. R. Shen, Nature **337**, 519 (1989).
[37] P. Guyot-Sionnest, J. H. Hunt, and Y. R. Shen, Phys. Rev. Lett. **59**, 1597 (1987).
[38] X. D. Zhu, H. Suhr, and Y. R. Shen, Phys. Rev. B **35**, 3047 (1987).
[39] T. C. Anglin and J. C. Conboy, Biophys. J. **95**, 186 (2008).
[40] T. C. Anglin and J. C. Conboy, Biochemistry **48**, 10220 (2009).
[41] K. L. Brown and J. C. Conboy, J. Am. Chem. Soc. **133**, 8794 (2011).
[42] J. Liu, K. L. Brown, and J. C. Conboy, Faraday Discuss. **161**, 45 (2013).
[43] K. L. Brown and J. C. Conboy, J. Phys. Chem. B **117**, 15041 (2013).
[44] V. Cheng, D. R. Kimball, and J. C. Conboy, J. Phys. Chem. B **123**, 7157 (2019).
[45] V. Cheng, R. Rallabandi, A. Gorusupudi, S. Lucas, G. Rognon, P. S. Bernstein, J. D. Rainier, and J. C. Conboy, Biophys. J. **121**, 2730 (2022).
[46] V. Cheng and J. C. Conboy, J. Phys. Chem. B **126**, 7651 (2022).
[47] J. Liu and J. C. Conboy, J. Am. Chem. Soc. **126**, 8894 (2004).
[48] J. Liu and J. C. Conboy, J. Phys. Chem. C **111**, 8988 (2007).
[49] T. C. Anglin, J. Liu, and J. C. Conboy, Biophys. J. **92**, L01 (2007).
[50] Y. R. Shen, *The Principles of Nonlinear Optics* (John Wiley and Sons, Inc., NJ, 1985).

19 December 2024 21:33:17

Published under an exclusive license by AIP Publishing

[51] B. Dick, A. Gierulski, G. Marowsky, and G. A. Reider, Appl. Phys. B: Photophys. Laser Chem. **38**, 107 (1985).
[52] J. Martín and S. Montero, J. Chem. Phys. **80**, 4610 (1984).
[53] D. Zhang, J. Gutow, and K. B. Eisenthal, J. Phys. Chem. **98**, 13729 (1994).
[54] C. Bolterauer and H. Heller, Eur. Biophys. J. **24**, 322 (1996).
[55] I. Burgess, M. Li, S. L. Horswell, G. Szymanski, J. Lipkowski, S. Satija, and J. Majewski, Colloids Surf., B **40**, 117 (2005).
[56] A. Tardieu, V. Luzzati, and F. C. Reman, J. Mol. Biol. **75**, 711 (1973).
[57] M. J. Janiak, D. M. Small, and G. G. Shipley, J. Biol. Chem. **254**, 6068 (1979).
[58] T. J. McIntosh and S. A. Simon, Biochemistry **32**, 8374 (1993).
[59] R. H. Pearson and I. Pascher, Nature **281**, 499 (1979).
[60] H. Eyring, Chem. Rev. **17**, 65 (1935).
[61] Y. R. Shen, Annu. Rev. Phys. Chem. **40**, 327 (1989).
[62] J. C. Conboy and M. A. Kriech, Anal. Chim. Acta **496**, 143 (2003).
[63] M. A. Kriech and J. C. Conboy, J. Opt. Soc. Am. B **21**, 1013 (2004).
[64] E. C. Y. Yan and K. B. Eisenthal, Biophys. J. **79**, 898 (2000).
[65] Y. Liu, E. C. Y. Yan, and K. B. Eisenthal, Biophys. J. **80**, 1004 (2001).
[66] J. S. Salafsky and K. B. Eisenthal, Chem. Phys. Lett. **319**, 435 (2000).
[67] J. H. Kim and M. W. Kim, J. Phys. Chem. B **112**, 15673 (2008).
[68] J. Zeng, H. M. Eckenrode, S. M. Dounce, and H. L. Dai, Biophys. J. **104**, 139 (2013).
[69] M. Sharifian Gh, M. J. Wilhelm, and H. L. Dai, J. Phys. Chem. Lett. **7**, 3406 (2016).
[70] L. K. Tamm and H. M. McConnell, Biophys. J. **47**, 105 (1985).
[71] D. Marsh, Biochim. Biophys. Acta, Rev. Biomembr. **1286**, 183 (1996).
[72] J. M. Taylor and J. C. Conboy, Biointerphases **19**, 031201 (2024).
[73] R. J. Tran, K. L. Sly, and J. C. Conboy, Annu. Rev. Anal. Chem. **10**, 387 (2017).
[74] R. J. Tran, M. S. Lalonde, K. L. Sly, and J. C. Conboy, J. Phys. Chem. B **123**, 4673 (2019).
[75] K. L. Sly and J. C. Conboy, Appl. Spectrosc. **71**, 1368 (2017).
[76] J. M. Smaby, V. S. Kulkarni, M. Momsen, and R. E. Brown, Biophys. J. **70**, 868 (1996).
[77] L. Qiao, A. Ge, Y. Liang, and S. Ye, J. Phys. Chem. B **119**, 14188 (2015).
[78] G. L. Gaines, *Insoluble Monolayers at Liquid-Gas Interfaces* (Interscience Publishers, New York City, 1996).
[79] C. h. Huang and J. T. Mason, Biochim. Biophys. Acta, Rev. Biomembr. **864**, 423 (1986).
[80] R. N. Ward, P. B. Davies, and C. D. Bain, J. Phys. Chem. B **101**, 1594 (1997).
[81] M. C. Henry, L. K. Wolf, and M. C. Messmer, J. Phys. Chem. B **107**, 2765 (2003).
[82] A. D. Quast, N. C. Wilde, S. S. Matthews, S. T. Maughan, S. L. Castle, and J. E. Patterson, Vib. Spectrosc. **61**, 17 (2012).
[83] R. A. Walker, J. C. Conboy, and G. L. Richmond, Langmuir **13**, 3070 (1997).
[84] J. Liu and J. C. Conboy, Vib. Spectrosc. **50**, 106 (2009).
[85] M. P. K. Frewein, P. Piller, E. F. Semeraro, K. C. Batchu, F. A. Heberle, H. L. Scott, Y. Gerelli, L. Porcar, and G. Pabst, J. Membr. Biol. **255**, 407 (2022).
[86] J. L. Slater, C. h. Huang, and I. W. Levin, Biochim. Biophys. Acta, Biomembr. **1106**, 242 (1992).
[87] T. C. Anglin, C. Michael, L. Hao, C. Katherine, and J. C. Conboy, J. Phys. Chem. B **114**, 1903 (2010).
[88] R. Homan and H. J. Pownall, Biochim. Biophys. Acta, Biomembr. **938**, 155 (1988).
[89] H. Raghuraman, S. Shrivastava, and A. Chattopadhyay, Biochim. Biophys. Acta, Biomembr. **1768**, 1258 (2007).
[90] A. Chattopadhyay, A. Chattopadhyay, E. London, and A. Chattopadhyay, Biochemistry **26**, 39 (1987).
[91] Sodium Hydrosulfite; CAS No.: 7775-14-6; Sigma-Aldrich, Saint Louis, MO, 2014.
[92] J. C. McIntyre and R. G. Sleight, Biochemistry **30**, 11819 (1991).
[93] M. Langner and S. W. Hui, Chem. Phys. Lipids **65**, 23 (1993).
[94] M. J. Moreno, L. M. B. B. Estronca, and W. L. C. Vaz, Biophys. J. **91**, 873 (2006).

19 December 2024 21:33:17

Published under an exclusive license by AIP Publishing